

# Spectra–Structure Correlations in the Near-infrared

L.G. Weyer<sup>1</sup> and S.-C. Lo<sup>2</sup>

<sup>1</sup>*Hercules Incorporated, Wilmington, DE, USA*

<sup>2</sup>*Merck & Co., Inc., West Point, PA, USA*

## 1 INTRODUCTION

It is generally thought that spectra–structure correlations are more difficult to make in the near-infrared (NIR) region of 700 nm ( $14\,290\text{ cm}^{-1}$ ) to 2500 nm ( $4000\text{ cm}^{-1}$ ) than the mid-infrared (MIR). Nevertheless, in view of the widespread application of NIR spectroscopic instruments to chemical analysis problems, it is important for practitioners to understand as much as possible of the relationship between NIR bands and chemical structure. A great deal is known about the band assignments in the NIR and a number of review articles are available.

NIR spectral absorption bands exist because the vibration of a chemical bond is not a simple harmonic motion. Due to the nonideal nature of a chemical bond, weaker overtones of bond vibrations occur at about one-half, one-third, one-quarter, and one-fifth the wavelength (or twice, three times, four times, and five times the frequency) of the fundamental vibration. The overtones of stretching vibrations are generally stronger than bending or rocking modes. The overtones observed primarily in the NIR region involve small hydrogen atoms coupled with larger atoms. There are two main reasons for this. One is that these vibrations are more anharmonic than those between atoms of similar size, and therefore have stronger overtones. The other is that the fundamental stretching vibrations of these C–H, O–H, and N–H bonds occur at the short-wavelength (high-frequency) end of the MIR spectrum due to their lower reduced mass. The proximity of these fundamentals to the NIR region means that their first overtones will occur in the NIR, while first overtones of other vibrations, such as C=O stretching and all of the bending and rocking modes,

occur within the MIR region. For example, the first overtone of a ketone's carbonyl stretch of  $1720\text{ cm}^{-1}$  is at about  $3440\text{ cm}^{-1}$ , which is still in the MIR. As each overtone is weaker by a factor of about 5–200 compared with the previous one, the second overtones are very weak compared with the first overtones.

The overtones of CH, OH, and NH bands have similar patterns to those in the MIR, although there are some interesting differences. These differences include self-cleaning and a wider separation with each overtone. The self-cleaning effect refers to minimization of symmetric vibrations, leaving the asymmetric bands more isolated.<sup>1</sup> Some bands appear to be further apart with each overtone because of anharmonicity considerations.<sup>2</sup> Also, most NIR bands are not necessarily broader than the corresponding MIR bands, although hydrogen-bonding effects do cause broadening in some overtones. Overlap with other bands such as those brought about by Fermi resonance may also cause some bands to appear broader.

If there were only overtone bands in the NIR, spectral interpretation would be simpler, and there would be less information available for both quantitative and qualitative analysis. However, the region also contains groups of combination bands of diminishing intensity. These bands involve hydrogenic vibrations almost exclusively, again because anharmonicity is important to their existence and their strength. These bands appear at frequencies that represent the sum of the two vibrations. The stronger combination bands involve good coupling between the two vibrations. According to Kaye,<sup>3</sup> good coupling is most likely to occur when the frequencies of the two vibrations are very similar or when they are bound together by a double bond or a ring. CH and OH combinations, therefore, may be weak unless the oxygen is bound to the carbon

that is participating in the CH stretching mode. The first and strongest set of combination bands appear in the NIR in the region of about 1900 nm ( $5260\text{ cm}^{-1}$ ) to 2500 nm ( $4000\text{ cm}^{-1}$ ).

Although combination bands are overlapped and difficult to assign, they provide much chemical information. For example, the aldehyde functional group, whose second overtone is difficult to see in the NIR, is easy to measure with a combination band due to the sum of a CH stretch and the carbonyl stretch at about  $4500\text{ cm}^{-1}$  or 2200 nm. It is not an isolated peak, however, as there may be several different types of CH bands that can couple with the carbonyl. It is also possible that infrared (IR) inactive vibrations can couple with an active one to create a combination band. Another complication is that one can also observe a doublet due to Fermi resonance when a fundamental band occurs close to an overtone or combination of another fundamental.<sup>4</sup>

Like MIR and Raman, NIR spectra can be used for kinetic studies and as a diagnostic tool. There are some reasonably isolated, useful spectral peaks present in the NIR region. Water, which is a very strong MIR and NIR absorber, has been measured in many different situations. Other examples include a well-isolated epoxy CH stretch first overtone, which has been used for curing studies,<sup>5</sup> and a primary amine combination band, which is useful for measurement of primary amines in the presence of secondary amines.<sup>6,7</sup>

While it may not be possible to understand the origin of all of the NIR spectral bands of even simple chemicals, it is important to attempt an understanding of the most important bands and to apply this knowledge to the development of quantitative analyses. Rapid NIR analyses, both in laboratories and in industrial processes, have become extremely important for process control, plant safety, quality control, rapid screening, patient monitoring, and many other situations. Most of these applications have been developed using statistically based chemometric techniques that can be employed without regard to spectral interpretation. Many times the user is taught to test the calibrations with prediction sets and not to bother with understanding the spectra.

There are several situations one can imagine where a purely statistical approach to calibration is not satisfactory. The calibration could be measuring something that correlates with the species of interest rather than the species itself. Measuring a hydrophilic fiber finish by measuring water peaks, for example, could lead to difficulties when unusual humidity conditions are encountered. Following a reaction by tracing water evolution instead of the starting material or the product could lead to a potential disaster when an ingredient is misfed. The water content could be fine, and the spectra may not look very different than

usual, but something could still be out of control. Spectral matching, exploration of spectral residuals, or discriminate analysis may help, but none of these are infallible. Understanding the spectra could also help in simplifying a calibration and in making it more robust. It could aid in feasibility studies and could prevent some expensive mistakes.

The identification of specific functional groups for the purpose of making sure that one is measuring the correct functionalities is only one aspect of the overall problem of understanding NIR calibrations. This would be the approach of choice if, for example, pure components or adequate model compounds are not available. One example would be measuring hydroxyl or acid number of complex polymers. Another approach would be to scan a spectrum of a pure component or model compound. Spectra of model compounds here or elsewhere<sup>8,9</sup> might be helpful. The next step would be to apply diagnostic techniques to the chemometric calibrations to determine how well the calibration for a specific constituent matches the spectrum of that substance.

Most chemometric calibrations fall into one of two classes: wavelength selection (as in stepwise multiple linear regression, filter selection, or genetic algorithm wavelength selection) and principal components-based methods, such as principal components regression (PCR) and partial least squares (PLS) of latent variables. Spectral interpretation can be applied to either of these approaches via two main methods. One is to examine the correlation or *R* plot, which provides a correlation value for the chemical or parameter being measured, at each wavelength. This plot shows where the most relevant bands exist for the measurement of interest within the matrix of the samples. It will not, therefore, look exactly like the spectrum of the raw material, but it should show some features of that spectrum. There may be negative correlation where interferences exist. If derivative data treatment is being used, the correlation plot will be more complex, but it will also probably have more points of high correlation (both positive and negative). In addition to aiding in wavelength selection or to understanding which wavelengths were selected, correlation plots have also been used to enhance PLS equation generation by providing information on the most relevant spectral regions so that regions that contain nothing but noise can be eliminated.

The second approach for applying spectral interpretation to chemometric calibrations is to examine the regression equation or beta coefficients from a PLS calibration. A plot of beta coefficients provides the final equation, which is used to calculate values for the component being measured. It is more useful than the individual loadings, which are often uninterpretable because they combine sources of variation with correlation. The plot of beta coefficients should also have some resemblance to the spectrum of the component itself, with some negative features where interferences

absorb. It is an important diagnostic that can tell the researcher when something is wrong with the calibration.

Correlation plots and regression coefficients may not exactly match model compounds, but again an understanding of the spectroscopy will provide additional insight. For example, there may be hydrogen-bonding effects occurring in the sample matrix that would prevent the diagnostic plots from resembling pure substances. Discussions and examples in this article may be helpful in explaining these spectral effects.

Spectral interpretation can also play a role in understanding chemometric calibrations of properties. Occasionally calibrations, especially PLS ones, are used to predict parameters such as fiber strength, hardness of wheat, or performance in an application test. Examination of the correlation plot or the regression equation ( $\beta$  coefficients) might provide some insight about the property, especially if some of the spectral bands can be assigned.

Band assignment information is also important as an aid in determining realistic limits of detection. For example, if a PLS calibration appears to be based mainly on one strong peak in a spectrum, and the basis of that absorption can be determined to be relevant to the component being measured, then an estimate can be made as to how much of the component can be measured relative to the noise level. A similar estimate can be made for a single-term multiple linear regression equation, at the primary measuring wavelength.

A body of information on NIR spectral bands does exist. Many overtone bands and some important combination bands have been identified, although there may be still some controversy in some interpretations. A large amount of band interpretations were made before the advent of chemometrics and “modern” NIR instrumentation and techniques, and these have been reviewed extensively in some classic articles of the 1950s and 1960s. These include those by Kaye,<sup>3</sup> Wheeler,<sup>10</sup> Goddu,<sup>11</sup> and Whetsel.<sup>12</sup>

Some recent review articles are also relevant. A review in 1985 brought the earlier works and some of the work from the 1970s and 1980s to the attention of practitioners of modern NIR.<sup>5</sup> A thorough review of interpretive NIR was published in 1996.<sup>13</sup> Some band assignment information is also available in the literature.<sup>4,14</sup>

It is difficult to make NIR absorption band assignments simply by multiplying or summing known fundamental frequencies because the overtone and combination bands are shifted by anharmonicity values. A number of semi-empirical methods have been used to assist in making the assignments. These include specific deuteration, chemical experiments such as dissolution in various solvents, two-dimensional (2D) correlation with IR spectra, difference spectra, 2D correlation of temperature series,<sup>15</sup>

spectral deconvolution, and exploring spectral residuals. 2D covariance spectroscopy was introduced by Barton *et al.*<sup>16,17</sup> to aid in the interpretation of NIR spectra of agricultural materials by comparing them with their MIR spectra. In this approach, a set of MIR and NIR spectra with varying compositions are obtained and their covariances are plotted and points of high correlation are noted. Noda *et al.*<sup>18</sup> used temperature-dependent spectral variations of Fourier transform near-infrared (FT-NIR) spectra to explore and assign NIR bands that are sensitive to temperature variation.

In the following sections, explanations of band assignments will be made wherever possible, and illustrations of the most important bands will be provided. All peak assignments have been rounded off for simplicity; a range of about 5–10 nm should be assumed for most general band assignments.

## 2 HYDROCARBONS

### 2.1 Aliphatic hydrocarbons

The carbon–hydrogen MIR fundamental stretching vibrations of aliphatic hydrocarbons lie in the region of 3000–2800  $\text{cm}^{-1}$ . In a general assignment, the first overtones of C–H stretching occur between 1700 and 1800 nm (5555–5882  $\text{cm}^{-1}$ ), the second overtones between 1150 and 1210 nm (8264–8696  $\text{cm}^{-1}$ ), and the third overtones between 880 (11 364  $\text{cm}^{-1}$ ) and 915 nm (10 929  $\text{cm}^{-1}$ ).<sup>10</sup> Although the CH force constant is the same for the three CH stretching modes, the  $\text{CH}_3$  (methyl),  $\text{CH}_2$  (methylene) and CH (methine) groups of saturated hydrocarbons occur at different wavelengths. The NIR spectra of selected alkanes in  $\text{CCl}_4$  are illustrated in Figure 1. The traditional designation of  $\nu$  for a stretching mode and  $\delta$  for a bending mode is used throughout the figures. In the hexane example, the first overtones of  $\text{CH}_3$  asymmetrical ( $\nu_a$ ) and symmetrical ( $\nu_s$ ) stretches occur near 1695 and 1705 nm (5907 and 5870  $\text{cm}^{-1}$ ), respectively. The asymmetric and symmetric  $\text{CH}_2$  stretching bands appear at about 1722 and 1762 nm (5807 and 5674  $\text{cm}^{-1}$ ), respectively.

In general, the intensity of methylene bands increases with increasing the chain length in most of hydrocarbons. Variations in the structure of the alkanes result in wavelength shifts and intensity changes. For example, an additional band was observed at 1771 nm (5646  $\text{cm}^{-1}$ ), which could be assigned to  $\text{CH}_3$  stretching in 2,5-dimethyl hexane. Tosi and Pinto<sup>19</sup> indicated that the terminal methyls have higher intensity than side methyls, and this is in agreement with the behavior of the fundamental CH stretching modes. In cyclic rings, there is a steady decrease in the  $\text{CH}_2$  asymmetric stretching wavelength from that of

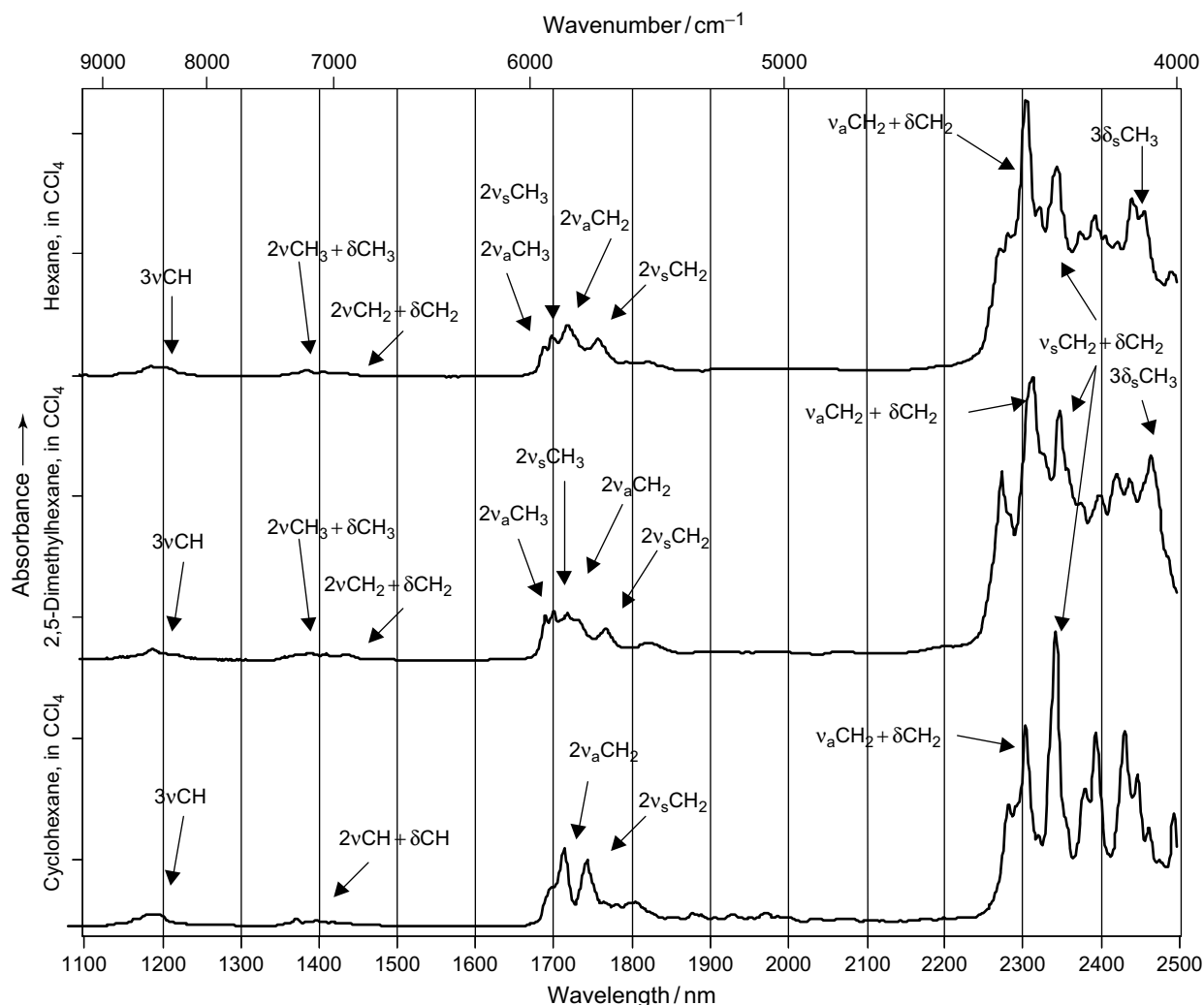


**Figure 1.** NIR spectra of selected alkanes. Note: all of the 1100–2500 nm spectra in  $\text{CCl}_4$ , except those of propionic acid and cumene hydroperoxide, were taken on a Bio-Rad FTS-40 FT-NIR using four-wavenumber resolution. The acid temperature series was obtained with a Bomem HOVAL FT-NIR. All others were done using a Varian Cary 5E in 1 nm resolution. At 1000 nm, 1 nm resolution corresponds to  $10\text{ cm}^{-1}$ ; at 2000 nm, it corresponds to  $2\text{ cm}^{-1}$ . Cell pathlengths varied from 0.01 to 10 cm.

cyclohexene to that of cyclopropane. As shown in Figure 1, the first overtone of cyclohexane reveals two strong bands at 1726 and 1755 nm. Bonanno and Griffiths<sup>20</sup> have assigned the two strong bands to asymmetric and symmetric  $\text{CH}_2$  stretching. Interaction between the two bands through Darling–Dennisen resonance causes a stronger intensity in the symmetric band. The stretching of the CH (methine) group in aliphatics is normally submerged by  $\text{CH}_3$  and  $\text{CH}_2$  strong absorptions.

The second overtone  $\text{CH}_3$  and  $\text{CH}_2$  asymmetrical stretching of *n*-alkanes appears at 1192 and 1210 nm ( $8389$  and  $8264\text{ cm}^{-1}$ ), respectively, as illustrated in Figure 2(a). Two additional partially resolved peaks with lower absorbance at 1153 and 1176 nm ( $8673$  and  $8503\text{ cm}^{-1}$ ) can be observed in higher-resolution measurements. These are due to the symmetrical stretch of  $\text{CH}_3$  and  $\text{CH}_2$ , respectively. In higher

alkanes above dodecane, the methyl group absorption is observed only as shoulder or inflection points on the predominant methylene absorption.<sup>21</sup> Due to the effect of anharmonicity for multiquanta transitions in higher vibrational modes ( $>$  second overtones), the band location and bandwidth do not behave as expected. The development of a “local mode model” as an alternative description for the higher vibrational energy states has been implicated on short wavelength NIR spectra and can be found in the literature.<sup>22,23</sup> The third overtones of C–H stretch of alkanes are at 912 and 929 nm ( $10965$  and  $10764\text{ cm}^{-1}$ ), and the fourth overtones are at 747 and 762 nm ( $13386$  and  $13123\text{ cm}^{-1}$ ), which resemble very closely the second overtone spectra (see hexane in Figure 3). These fairly simple spectral features could be attributed to the local mode behavior of the higher excited vibrations. Even in difficult

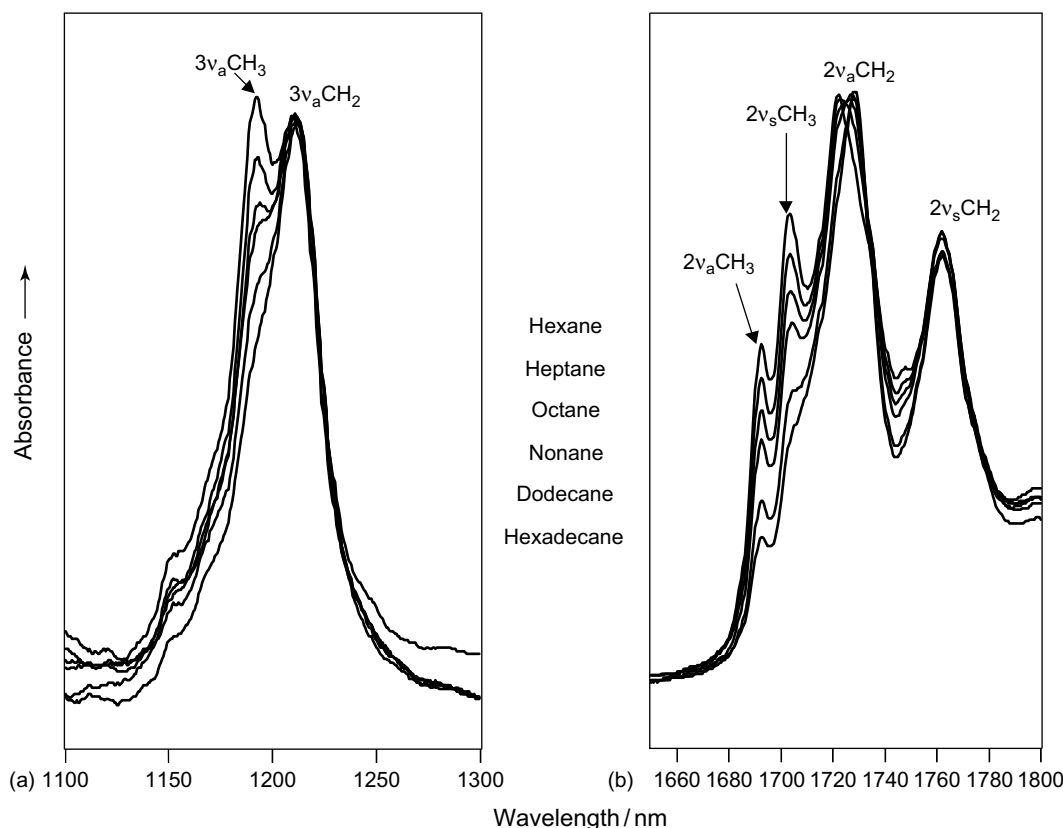


**Figure 2.** NIR spectra of *n*-alkanes in the CH stretch first and second overtone regions. Note: the curves represent hexane through hexadecane, from top to bottom.

cases of band assignments, the C–H stretch of cyclohexane, for example, becomes much simpler in the higher excitation states.

The combination bands are usually difficult to assign to precise pairs of vibration modes from fundamental and deformation (bending) modes. As shown in the spectrum of hexane in  $\text{CCl}_4$  in Figure 1, the regions of 1300–1500 nm ( $6666\text{--}7690\text{ cm}^{-1}$ ) and 2200–2500 nm ( $4000\text{--}4545\text{ cm}^{-1}$ ) could be assigned as CH combination bands. Two sharp peaks have been assigned to  $2 \times \text{CH}$  stretch and CH bending of both  $\text{CH}_2$  and  $\text{CH}_3$  groups at about 1392 and 1412 nm ( $7184$  and  $7082\text{ cm}^{-1}$ ), respectively. The combination bands in the range of 2000–2500 nm ( $5000\text{--}4000\text{ cm}^{-1}$ ) exhibit complex spectral features with high absorbances. Full interpretation of structure–spectral correlations is a difficult challenge, but the spectral features are of particular value in qualitative analysis. The two strongest bands near 2307 and 2347 nm ( $4334$  and  $4260\text{ cm}^{-1}$ ) have been assigned to the asymmetric and symmetric modes of the combination of CH stretch and  $\text{CH}_2$  bending motions.<sup>24</sup> The symmetric combination of stretch and bending modes interacts with the second overtone of  $\text{CH}_2$  bending modes through Darling–Dennison resonance. Other absorptions between 2380 and 2440 nm ( $4100$  and  $4200\text{ cm}^{-1}$ ) are

possibly due to the combinations of CH stretching modes and wagging and higher frequency modes.

## 2.2 Aromatics

The aromatic CH stretch produces several bands at shorter wavelengths than the aliphatic CH absorptions. As shown in Figure 4 for benzene in  $\text{CCl}_4$ , the major NIR absorption bands are at 1140 nm ( $8772\text{ cm}^{-1}$ ), 1670 nm ( $5988\text{ cm}^{-1}$ ), 2150–2180 nm ( $4651\text{--}4587\text{ cm}^{-1}$ ) and 2460 nm ( $6065\text{ cm}^{-1}$ ). The major peak at 1670 nm ( $5988\text{ cm}^{-1}$ ) has been assigned to the first overtone of the CH stretch and has been confirmed by comparison of the spectrum of  $\text{C}_6\text{D}_6$ .<sup>25</sup> This statement is an oversimplification, however. As described by Kaye,<sup>3</sup> the peak near 1670 nm is a doublet and represents combinations of four individual fundamental bands, only one of which is IR active. All involve CH stretching.<sup>26</sup>

In high-resolution optothermal spectra, two main peaks located around 1132 and 1140 nm ( $8834$  and  $8772\text{ cm}^{-1}$ ) are seen, which represent the real CH second overtone and a combination band, respectively.<sup>27</sup> The third overtone is at 874 nm ( $11442\text{ cm}^{-1}$ ) in liquid benzene, but shifts to

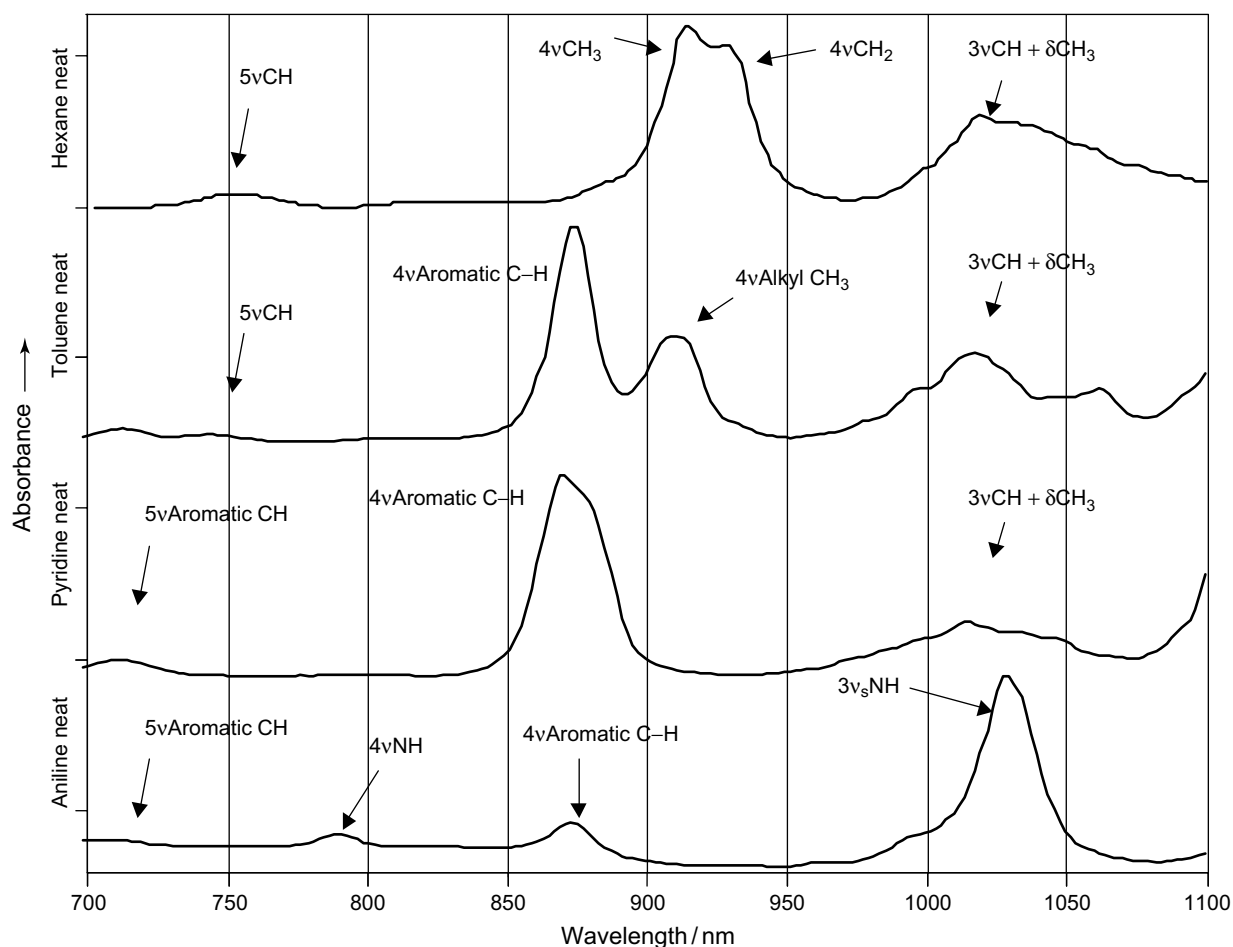


**Figure 3.** NIR spectra of selected hydrocarbons and amines in the short-wavelength region.

880 nm ( $11\,364\text{ cm}^{-1}$ ) in  $\text{CCl}_4$ , and the fourth overtone of aromatic CH occurs at 714 nm ( $14\,000\text{ cm}^{-1}$ ). A strong peak at 2460 nm ( $4065\text{ cm}^{-1}$ ) has been assigned as due to the combination band of CH stretching and HCC bending (benzene's IR peak at  $1030\text{ cm}^{-1}$ ). The CH stretching peak involved in this combination is IR inactive. The bands near 2140 nm ( $4675\text{ cm}^{-1}$ ) have been assigned to combinations of (IR-inactive) CH stretching and ring stretching (the benzene IR peak at  $1470\text{ cm}^{-1}$ ).<sup>25</sup>

Alkyl benzenes show spectral features of both aromatic and aliphatic hydrocarbons. The patterns are more complicated due to the reduction of benzene symmetry and the presence of two types of CH stretching vibrations. As shown in the spectrum of toluene in Figure 4, the CH first overtone band at 1680 nm ( $5952\text{ cm}^{-1}$ ) is broader than the peak in the benzene spectrum. The broadness of the overtone peak in toluene is due to the contributions from both the aromatic and aliphatic CH stretches. Additional alkyl groups in xylenes or propylbenzene also produce a displacement of the CH overtone band to longer wavelength due to their electropositive nature.

As compared with the benzene peak near 2460 nm ( $4065\text{ cm}^{-1}$ ), two bands are observed in the mono-, di- and trisubstituted methylbenzenes. Only a single band could be observed in higher substituted methylbenzenes (e.g. durene, penta- and hexamethylbenzene). Luty and Rohleder<sup>28</sup> suggested that the band at 2451 nm ( $4080\text{ cm}^{-1}$ ) corresponds to the second overtone of symmetric bending  $\text{CH}_3$  vibrations. A linear relationship is found between the number of methyl groups substituted into the benzene ring and the intensity of characteristic absorption bands. The bands near 2451 nm ( $4080\text{ cm}^{-1}$ ) yield more accurate results for the derivatives containing one to four methyl groups. In higher substituted methylbenzenes, the first overtone band at 1767 nm ( $5660\text{ cm}^{-1}$ ) provides better prediction. In a comprehensive investigation of NIR absorptions using photoacoustic experiments, the tentative assignments of 11 substituted benzenes have been reported.<sup>29</sup> With regard to higher vibrational states, the second overtone of the CH stretch in alkylated benzenes occurs at 1145 nm ( $8734\text{ cm}^{-1}$ ), while the alkyl CH stretch occurs at 1192 nm ( $8389\text{ cm}^{-1}$ ). Approximately 5–10 nm displacements were observed into longer

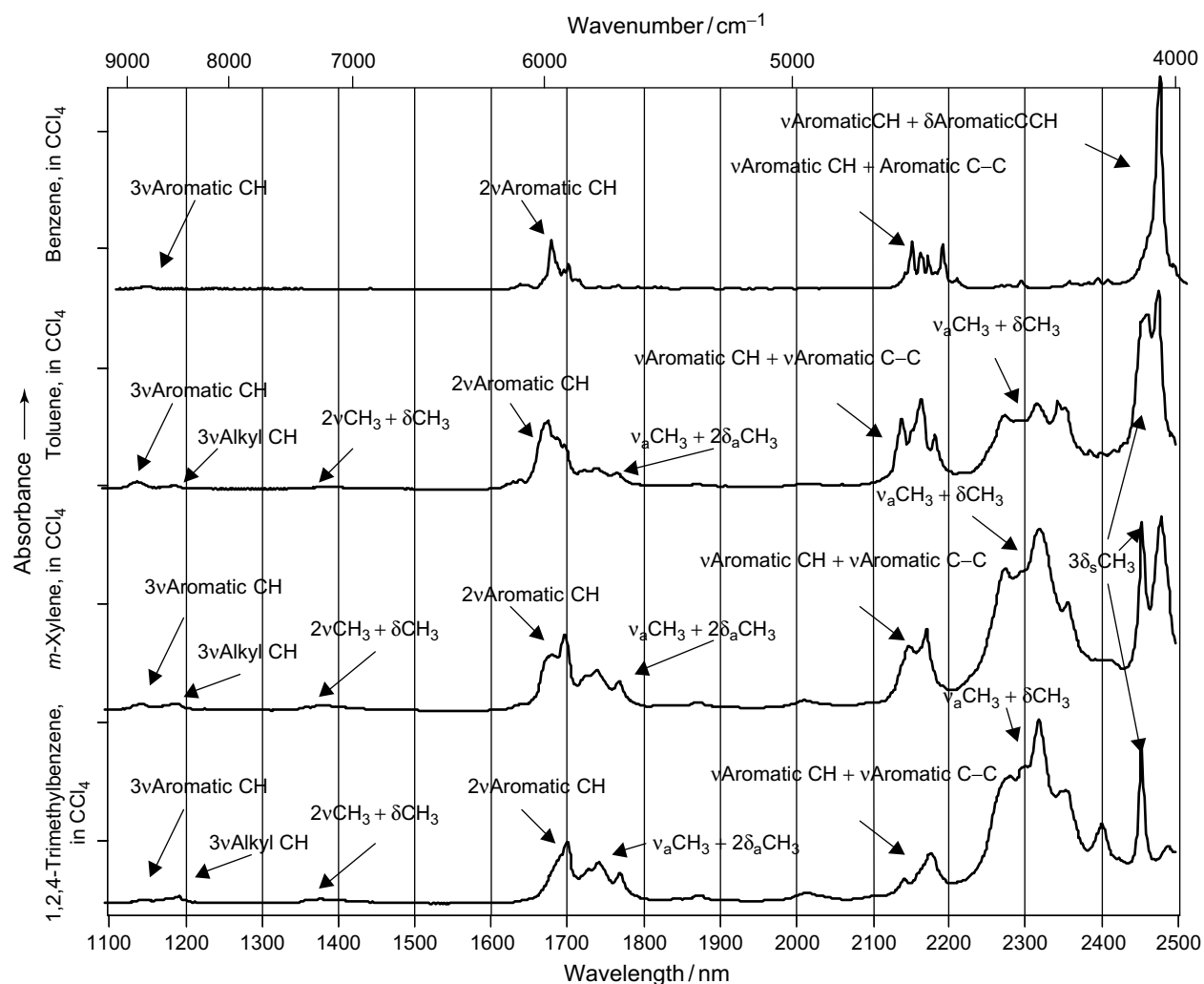


Figure 4. NIR spectra of selected aromatics.

wavelength as compared with benzene's second CH overtone band. However, the displacement is small on the third, fourth and fifth overtones of alkyl-substituted benzenes.

The displacements of overtone absorption among different polar substituents on benzene also give some qualitative information. As shown in Figure 5, electronegative groups such as halogens or nitro groups produce displacements to lower wavelength, while electropositive substituents (alkyl group) generate a displacement to longer wavelength. The CH overtones of heterocyclic aromatic rings also give slightly different wavelength shifts from the normal aromatic values. For example, the similarity of the overtone transitions of benzene and pyridine has also been studied extensively.<sup>30</sup> The liquid-phase spectrum of pyridine displays two broad absorptions in the overtone spectrum. It appears that the presence of the electron-attracting nitrogen atom in the ring splits the absorption into two peaks. The bands at 1704 and 1714 nm (5867 and 5835 cm<sup>-1</sup>)

may be assigned to the first overtone CH stretching at the 2,6-positions [C(2)–H and C(6)–H], while the bands at 1679 and 1693 nm (5956 and 5907 cm<sup>-1</sup>) are due to the 3,5-position of CH first overtones, respectively. The next strong band, at 1669 nm (5992 cm<sup>-1</sup>), has been assigned to a combination band involving the CH at the 2,6-position.<sup>31</sup> The two bands appearing at 1138 and 1156 nm (8785 and 8651 cm<sup>-1</sup>) are assigned to the second overtone. The third and fourth overtones also show similar bands at 872 and 885 nm (11474 and 11296 cm<sup>-1</sup>) and 712 and 724 nm (14037 and 13810 cm<sup>-1</sup>), respectively, as shown in Figure 3. The longer wavelength band was assigned to CH stretches at the 2 and 6 positions and the shorter wavelength band was attributed to the CH stretches at the 3, 4, and 5 positions.<sup>32</sup>

In the study of methyl-substituted pyridines, the aryl regions of the overtones show a simplified structure having one peak progression for each nonequivalent

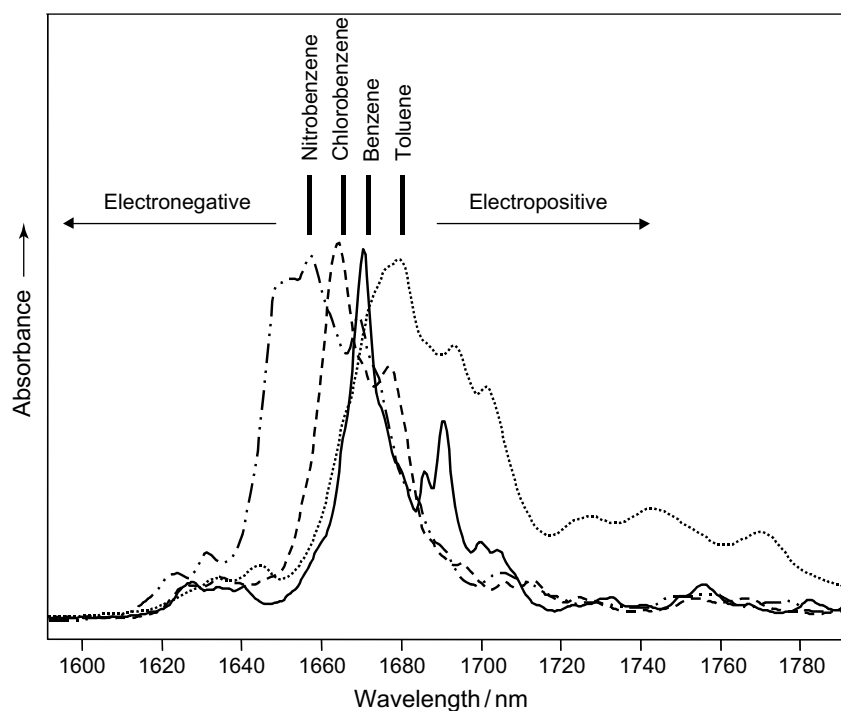


**Figure 5.** Displacement effects of polar substituents on aromatic compounds.

CH. According to a recent investigation,<sup>33</sup> these peak progressions are best described as uncoupled anharmonic Morse oscillators. In addition, the methyl regions of the methylpyridines show complex profiles. The band profile in 3- and 4-methylpyridine is similar to that of toluene, since the methyl groups of these compounds are free rotors and all have a low energy barrier to rotation. However, the methyl band profiles of 2-methylpyridine are complex, and these patterns indicate that vibration-torsional coupling is an important contributor to the complex structure.<sup>33</sup>

### 2.3 Olefins

Several variations in olefinic CH stretch first overtones occur in the NIR region. The asymmetric  $=CH_2$  stretching appears from 1615 to 1636 nm ( $6190$ – $6110\text{ cm}^{-1}$ ), while the symmetric  $=CH_2$  appears at about 1637 nm ( $6110\text{ cm}^{-1}$ ). The  $=CH$  stretching of a  $=CHR$  group also occurs at 1600 nm ( $6250\text{ cm}^{-1}$ ) and is dependent upon the type of R group. For example, vinyl ethers ( $CH_2=CH-O-$ ) absorb at a shorter wavelength of about 1615 nm ( $6192\text{ cm}^{-1}$ ), but the  $\alpha,\beta$ -unsaturated ketones absorb at the slightly longer wavelength of 1620 nm ( $6173\text{ cm}^{-1}$ ). Yalvac *et al.*<sup>34</sup> found that the asymmetric  $=CH_2$  stretch in the 1623–1644 nm ( $6080$ – $6160\text{ cm}^{-1}$ ) region shifts towards longer wavelengths and decreases in the intensity of the band with increasing chain length for

monoalkylated light alkenes. The decrease of the dipole moment change of the molecule due to the increased chain length may explain the intensity decrease. Gassman and Hooker<sup>35</sup> have tabulated the CH first overtones of a collection of norbornene-type compounds, showing the effects of skeletal structure, degree of substitution, and the electronic and stereochemical effects of substituents.

A combination band occurs near 2140 nm. Holman and Edmondson<sup>36</sup> have observed the combination band at 2140 nm ( $4673\text{ cm}^{-1}$ ) as a clear indicator to differentiate cis/trans unsaturation structure in nonconjugated fatty acids. Trans double bonds do not absorb at 2140 nm and thus this information could be used to determine the content of cis double bonds of natural fats and oils. Yalvac *et al.*<sup>34</sup> also showed the characteristic absorption at 2140 nm ( $4673\text{ cm}^{-1}$ ), and additional bands near 1661 nm ( $6020\text{ cm}^{-1}$ ) and 2170 nm ( $4600\text{ cm}^{-1}$ ) in the spectra of cis dialkylated alkenes, but not in that of the trans isomers. The methyne  $\equiv C-H$  stretching vibration has a strong and sharp overtone band at 1530 nm ( $6536\text{ cm}^{-1}$ ).

## 3 AMINES AND AMIDES

The NIR spectra of primary, secondary and tertiary amines are unique and can be differentiated from each other. The first overtone of the NH stretch of primary amines has two bands between 1450 nm ( $6897\text{ cm}^{-1}$ ) and 1550 nm ( $6452\text{ cm}^{-1}$ ) due to coupling.<sup>37</sup> As shown in the example of



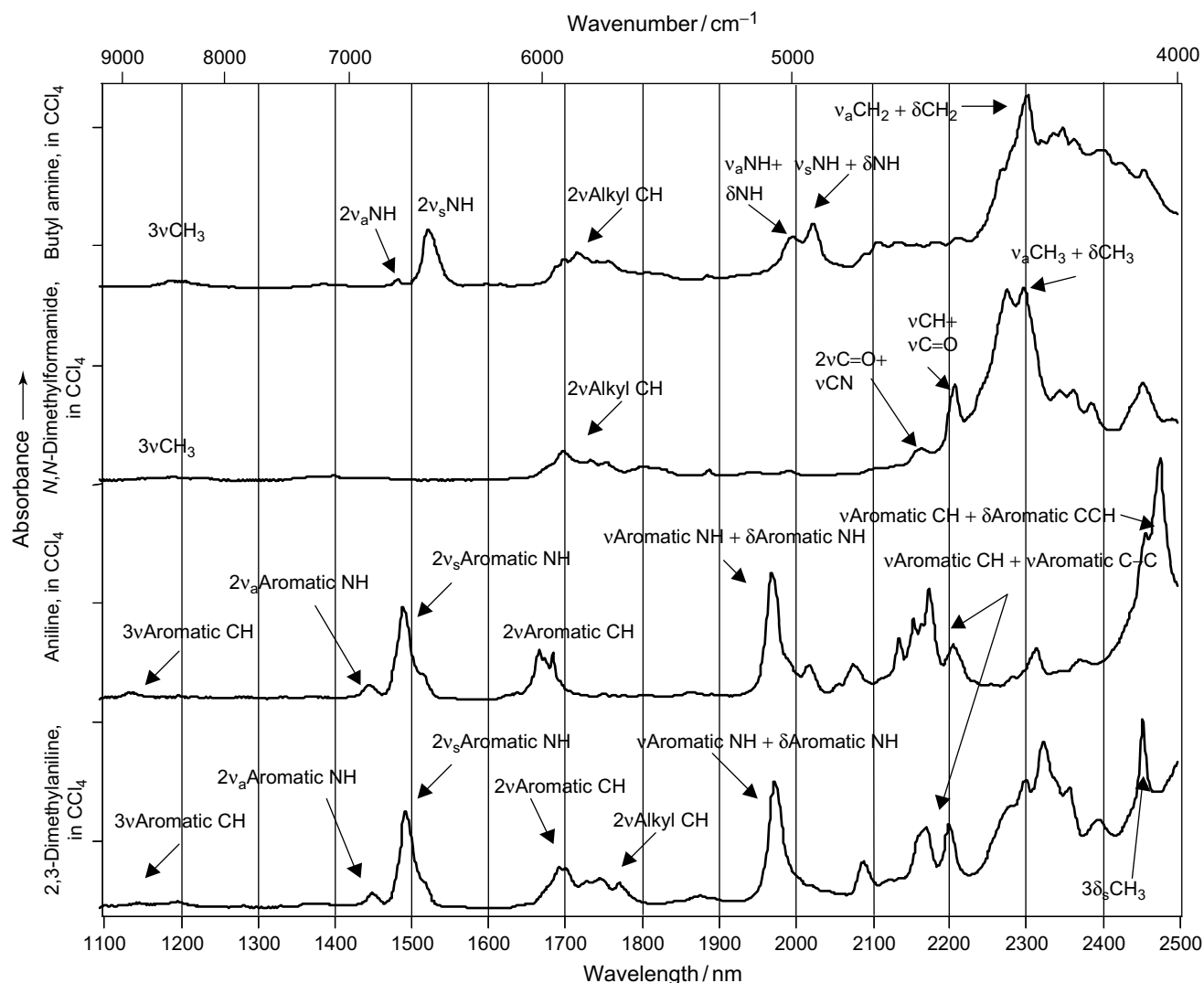


**Figure 6.** NIR spectra of selected amines and an amide.

butyl amine in Figure 6, two bands due to asymmetric and symmetric NH stretching occur at 1486 and 1526 nm ( $6730$  and  $6553\text{ cm}^{-1}$ ), respectively. The figure illustrates amines in dilute carbon tetrachloride solution, and the NH stretch first overtones broaden and shift to longer wavelengths with an increase in concentration. The symmetric absorption of the  $-\text{NH}_2$  group is much more intense ( $\sim 6\text{--}7$  times) than the asymmetric absorption.<sup>38</sup> A single peak that occurs near  $1030\text{--}1040\text{ nm}$  ( $971\text{--}962\text{ cm}^{-1}$ ) has been assigned to the second overtone of  $-\text{NH}_2$ . The third overtone occurs as a doublet at  $806$  and  $779\text{ nm}$  ( $12407$  and  $12837\text{ cm}^{-1}$ ). The absorption of the latter band is also stronger, and its intensity increases with increasing chain length. The fourth overtone appears as a doublet near  $661\text{ nm}$  ( $15129\text{ cm}^{-1}$ ), but with lower intensity.<sup>12</sup>

The first and second overtones of secondary amines have only one band near  $1540\text{ nm}$  ( $6494\text{ cm}^{-1}$ ) and  $1000\text{ nm}$

( $10000\text{ cm}^{-1}$ ), respectively. The tertiary amines have no NH absorptions in the overtone region, but only one peak occurs near  $1260\text{--}1270\text{ nm}$  ( $7937\text{--}7874\text{ cm}^{-1}$ ), which may be assigned to a combination of CH and CN stretching modes.

In addition, primary amines have bands near  $1990$  and  $2020\text{ nm}$  ( $5025$  and  $4950\text{ cm}^{-1}$ ), which have been found to be related to amines in different environments.<sup>39</sup> These bands can be characterized as the combination of NH stretching and bending vibrational modes, and are absent in secondary and tertiary amines. The band near  $1990\text{ nm}$  is prominent in hexane solutions of primary amines, while the band near  $2020\text{ nm}$  increases upon addition of more polar solvents such as chloroform.<sup>40</sup> The carbon tetrachloride spectrum shown in Figure 6 shows both bands. The sensitivity of this band to solvent polarity has been attributed to the bending (scissoring) vibration, which is

similarly sensitive in the MIR region. This pair of combination bands has been useful in studying amine interactions and also in quantitative analyses of mixtures of amines.

In heterocyclic amines such as pyrroles, indoles and carbazoles, there is an intense first overtone NH stretching between 1440 nm ( $6897\text{ cm}^{-1}$ ) and 1470 nm ( $6803\text{ cm}^{-1}$ ).<sup>41</sup> It can be used for qualitative detection of heterocyclic NH compounds. Another special case of amine is ammonia in water,  $\text{NH}_4\text{OH}$ . Ammonia in water shows strong bands at 1534 nm ( $6520\text{ cm}^{-1}$ ), 2000 ( $5000\text{ cm}^{-1}$ ), and 2210 nm ( $4525\text{ cm}^{-1}$ ) in addition to water bands.<sup>42</sup> The first is an NH stretch first overtone, while the other two are combinations.

The NH stretching bands of aromatic amines show a doublet in the first overtone region, but it is shifted to lower wavelengths relative to aliphatic amines. Figure 6 shows the NIR spectrum of aniline in  $\text{CCl}_4$ . The asymmetric vibration occurs at 1450 nm ( $6897\text{ cm}^{-1}$ ) and the symmetric band is in the region of 1492 nm ( $6702\text{ cm}^{-1}$ ). The band at 1972 nm ( $5071\text{ cm}^{-1}$ ) is due to a combination of NH stretching and bending, while the weak second overtone NH symmetric band can be observed at 1020 nm ( $980\text{ cm}^{-1}$ ), as shown in Figure 3. Thus, the aromatic amines can be resolved from aliphatic primary and secondary amines. In studies of ring-substituted derivatives, Whetsel<sup>43</sup> has investigated the correlation of substituent electronic nature with band positions and intensities in both NH stretching and combination modes. The shifts of NH overtone bands may be observed as effects of various solvents and temperature conditions. The effects of hydrogen bonding on the mechanical anharmonicity of the NH stretching vibration have been reported. Weak hydrogen bonding appears to decrease the anharmonicity of the vibration resulting in the change of peak width in the overtone absorptions.<sup>44</sup>

NIR spectra of primary amides ( $\text{RCO-NH}_2$ ), such as formamide, acetamide and benzamide, have been studied in chloroform solution.<sup>45</sup> Two bands at 1430 nm ( $6995\text{ cm}^{-1}$ ) and 1490 nm ( $6710\text{ cm}^{-1}$ ) have been assigned to first overtones of the asymmetric and symmetric N–H stretching modes. A single combination band of symmetric and asymmetric NH fundamental stretching appears at 1470 nm ( $6805\text{ cm}^{-1}$ ). Several bands near 1960 and 2030 nm ( $5100$  and  $4925\text{ cm}^{-1}$ ) were assigned to the combinations of fundamental NH stretch and amide II and III deformations (these MIR bands are generally considered to be due to different types of coupling of the CNH deformation and CN stretch). For example, a strong band at 1960 nm ( $5100\text{ cm}^{-1}$ ) was assigned to the combination of asymmetric NH stretching with amide II. Two weak bands at 2030 ( $4925\text{ cm}^{-1}$ ) and 2010 nm ( $4975\text{ cm}^{-1}$ ) were attributed to the combination of asymmetric NH stretching with amide III and symmetric NH stretching with amide

III, respectively. The second overtone of primary amides occur at 975–989 nm ( $10\,110$ – $10\,260\text{ cm}^{-1}$ ).

The assignment of secondary amides has also been studied extensively. A single band near 1470–1490 nm ( $6803$ – $6711\text{ cm}^{-1}$ ) for *N*-methylacetamide and other simple amides was attributed to the first overtone NH stretches. The combination bands in the range of 2000–2020 nm ( $4950$ – $5000\text{ cm}^{-1}$ ) and 2110–2130 nm ( $4695$ – $4740\text{ cm}^{-1}$ ) were assigned to the fundamental NH stretch with amide II and fundamental NH stretch with amide III, respectively. An additional band at 2160 nm ( $4630\text{ cm}^{-1}$ ) was attributed to the combination band of the first overtone of C=O with amide III ( $2\nu_{\text{C=O}} + \text{amide III}$ ). However, other researchers suggested that this band could not be attributed to an NH mode.<sup>46</sup> Upon deuteration, these combination bands were reduced in intensity on selected *N*-*d*-amides. Therefore, Krikorian and Mahpour<sup>45</sup> concluded that the amide assignment was substantiated. The tertiary amides lack the NH absorptions observed in the primary and secondary amides, except for a band at 2139 nm ( $4675\text{ cm}^{-1}$ ) for *N,N*-dimethylformamide, at 2151 nm ( $4650\text{ cm}^{-1}$ ) for *N,N*-dimethylacetamide, and at 2160 nm ( $4630\text{ cm}^{-1}$ ) for *N,N*-dimethylbenzamide. These bands correspond to the combination band of  $2\nu_{\text{C=O}} + \text{amide III}$ . The second overtone of secondary amides occurs near 981 nm ( $10\,194\text{ cm}^{-1}$ ).

## 4 HYDROXYLS

### 4.1 Alcohols

The most important features in the NIR spectra of alcohols are the first overtone of the OH stretch, the second overtone, and a combination band near 2100 nm ( $4760\text{ cm}^{-1}$ ). The first overtone in particular has been studied by a number of researchers, and has been employed for hydrogen bonding studies. The band is apparently quite complex, as the monomer and several hydrogen-bonded structures are possible.

In a dilute solution of a non-hydrogen-bonding solvent or at high temperature, aliphatic alcohols have a first overtone peak at about 1410 nm ( $7090\text{ cm}^{-1}$ ). Some examples are shown in Figure 7. This peak is a doublet for *n*-butanol, for example, due to rotational isomers.<sup>47</sup> The peak may also be split due to interactions with the electrons of phenyl rings or halogens, as in benzyl alcohol, for example. In hydrogen-bonded alcohols, there is a broad peak in the 1460–1600 nm region ( $6850$ – $6240\text{ cm}^{-1}$ ), which has been generally attributed to the first overtone of the hydroxyl. This bonded OH peak appears to be broader as a first overtone when compared with its fundamental, as was observed in a series of spectra taken at different

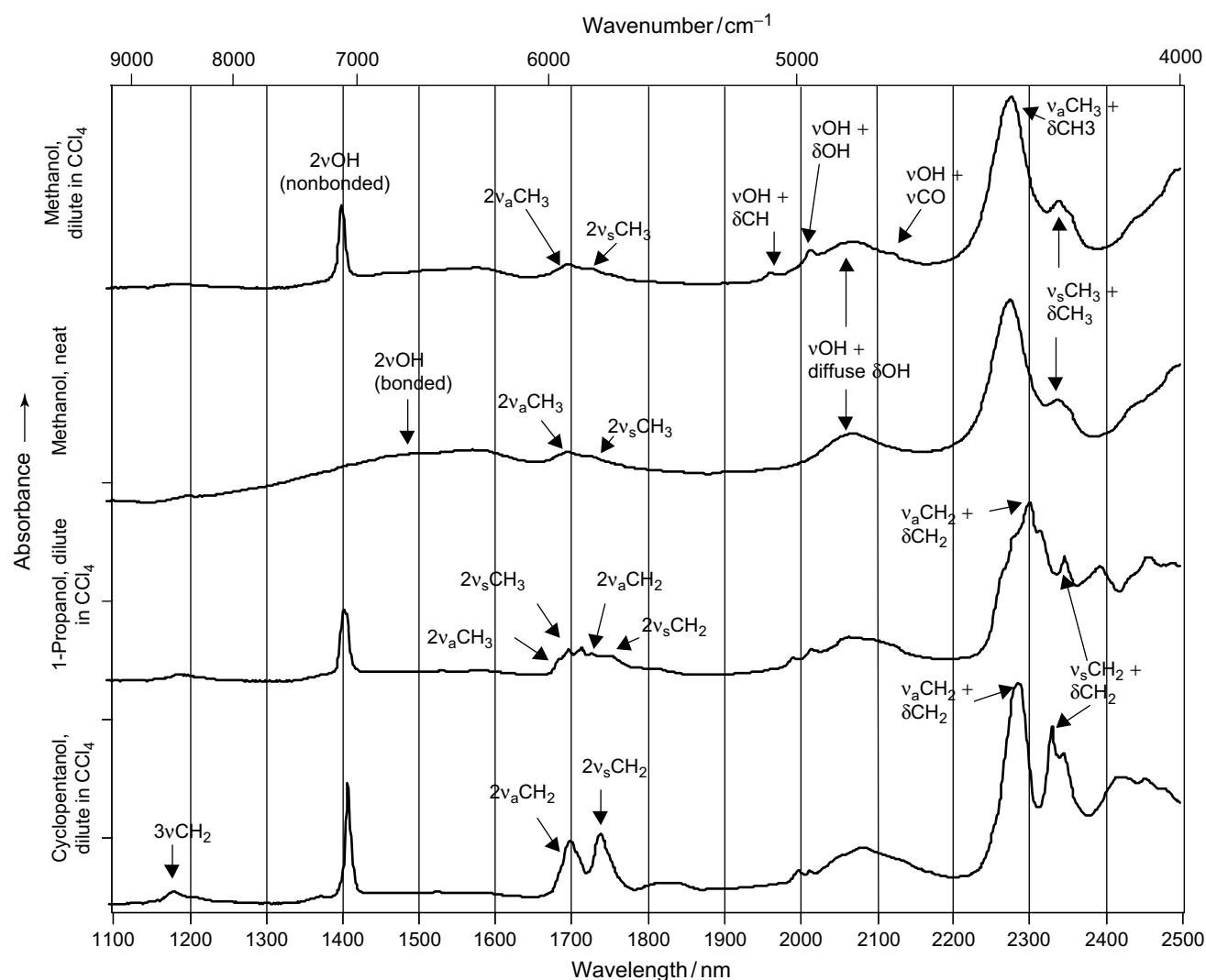


Figure 7. NIR spectra of selected alcohols.

temperatures.<sup>48</sup> On the other hand, the nonbonded OH first overtone is stronger relative to the bonded species than it is in the fundamental, and can be readily detected even when not visible in the fundamental region.<sup>49</sup>

However, there is some confusion over whether combinations of OH stretch and CH stretch in the 1580-nm ( $6330\text{ cm}^{-1}$ ) region contribute to the broad peak.<sup>3,50</sup> Although Kaye appears to assign the 1580-nm peak to this combination, he also claims that combination bands involving CH stretch and OH stretch are very weak because stretching vibrations involving different atoms do not couple well unless their frequencies are nearly the same or the groups involve double bonds or rings. Kaye's apparent assignment may be simply a function of how one reads his chart, as the two small OH/CH peaks observable in his dilute  $\text{CCl}_4$  spectrum overlap the broad, bonded OH stretch first overtone. Bell and Barrow<sup>51</sup> show that the

small peaks (one in ethanol and two in methanol, due to coupling with asymmetric and symmetric CH stretch) are not present in  $\text{CD}_3\text{OH}$  dissolved in carbon tetrachloride. Czarnecki *et al.*<sup>15</sup> suggest that the series of peaks between 1410 nm ( $7100\text{ cm}^{-1}$ ) and 1600 nm ( $6240\text{ cm}^{-1}$ ) are all due to OH stretch first overtones of different aggregates, such as monomer, dimers, and polymers of the alcohols. Czarnecki *et al.* found that the 1570-nm peak decreases with temperature when the monomeric 1410-nm peak increases, which supports their theory that it is due primarily to OH overtones. There are apparently contributions from both hydroxyl overtones and CH/OH combinations involved in the broad envelope, although the bonded OH first overtone probably predominates. The evidence of Davies and Rutland<sup>50</sup> does not contradict this statement.

Hydrogen bonding of alcohols with solvents occurs to different extents in different matrices. The spectra of

methanol in a series of solvents from carbon tetrachloride through pyridine have been studied.<sup>51,52</sup> The first overtone region exhibits two major peaks when an alcohol is in a solvent capable of hydrogen bonding. Bell and Barrow have shown that these two peaks are not affected by temperature or dilution (except for the formation of dimer at very high concentrations). They also show that the second peak is not due to an OH/CH combination band. They suggest that the two peaks are both monomeric hydrogen-bonded alcohol first overtones, and that the vibrational energy level has been split into two, creating a double minimum in the potential energy curve.

In dilute solution, primary, secondary, and tertiary hydroxyls have slightly different peak positions. This is shown in Figure 8, an expansion of a series of butanols in carbon tetrachloride. Note also that the primary and secondary hydroxyls show signs of the doublet ascribed by Czarnecki to be due to rotational isomers.

The second overtone of the nonbonded OH stretch occurs at about 960 nm ( $10\,400\text{ cm}^{-1}$ ), and the third at about 740 nm ( $13\,500\text{ cm}^{-1}$ ) for simple alcohols. The second overtone has also been used for a number of hydrogen-bonding studies.<sup>10</sup> Variations in the structure of the alcohol result in splitting of the band and systematic shifts. Second overtones of OH stretch appear to have less interference from CH combination bands than first overtones and can therefore be more useful for thermodynamic studies.<sup>52</sup> Additional overtones of the nonbonded hydroxyl stretch of alcohols, using gaseous ethanol as a model, are the fourth overtone at 735 nm ( $13\,600\text{ cm}^{-1}$ ), the fifth at 600 nm ( $16\,700\text{ cm}^{-1}$ ), and the sixth at 510 nm ( $19\,500\text{ cm}^{-1}$ ).<sup>53</sup> Additional bonded hydroxyl bands are the OH stretch second overtone at 1047 nm ( $9550\text{ cm}^{-1}$ ), a combination of the first overtone of the OH stretch and twice the methyl CH

deformation at 1065 nm ( $9386\text{ cm}^{-1}$ ), and a combination of the OH stretch first overtone plus three times the CO stretch at 1029 nm ( $9720\text{ cm}^{-1}$ ).<sup>54</sup>

A distinctive combination region of alcohols occurs between 1800 and 2200 nm ( $5550\text{--}4550\text{ cm}^{-1}$ ). In the dilute solution spectrum of methanol, three sharp peaks are observed superimposed on a broader continuum. The sharp peaks have been assigned to OH stretch plus CH bending at 1965 nm ( $5090\text{ cm}^{-1}$ ), OH stretch plus OH bending at 2017 nm ( $4960\text{ cm}^{-1}$ ), and OH stretch plus CO stretch at 2124 nm ( $4710\text{ cm}^{-1}$ ).<sup>3</sup> There is also a second combination of OH stretching and a different OH bending mode at about 2520 nm ( $3970\text{ cm}^{-1}$ ). These sharp peaks are at different positions in other alcohols, as shown in Figure 7. In the neat spectrum, these peaks become one broad band centered at about 2100 nm. In the MIR, a diffuse OH association band related to deformation occurs at about  $1420\text{ cm}^{-1}$ , which can account for the 2100-nm NIR band ( $1420\text{ cm}^{-1} + 3350\text{ cm}^{-1} = 4770\text{ cm}^{-1}$ , corresponding to about 2100 nm). This diffuse band is said to disappear in dilute solutions of alcohols in the MIR, where hydrogen bonding does not occur.<sup>55</sup>

## 4.2 Phenols

Phenols show absorptions in the same regions as aliphatic alcohols, with first overtones near 1400–1440 nm and combination bands near 2000 nm. As seen in Figure 9, the first overtone of phenol itself in  $\text{CCl}_4$  is a single peak at 1420 nm ( $7040\text{ cm}^{-1}$ ), but orthohalogens show a doublet due to cis/trans isomerism where the cis form is stabilized by internal hydrogen bonding between the hydroxyl and the halogen.<sup>10,56</sup> The second overtone of dilute phenol in carbon tetrachloride is at 1000 nm ( $10\,000\text{ cm}^{-1}$ ) and the third at 750 nm ( $13\,250\text{ cm}^{-1}$ ).

Due to the difference in acidity of phenol relative to simple aliphatic alcohols, its spectra in different solvents are quite different from those of methanol and ethanol.<sup>51</sup> In solvents of low hydrogen-bonding capability, phenol shows both free and bonded OH first overtones because the solvent cannot bond the phenol completely. In solvents that are more capable of hydrogen bonding, phenol behaves like the alcohols, except that the sequence is accelerated; for example, the spectrum of phenol in *N,N*-dimethylformamide appears similar to the spectrum of ethanol in pyridine.

In a study of combination bands of various halogenated phenols, Wulf *et al.*<sup>56</sup> found that most of the combinations involved the OH and bending or twisting modes of the aromatic ring or the OH group itself. This conclusion was based on the observation that pentachlorophenol, which had no CH groups, showed very similar patterns to the other

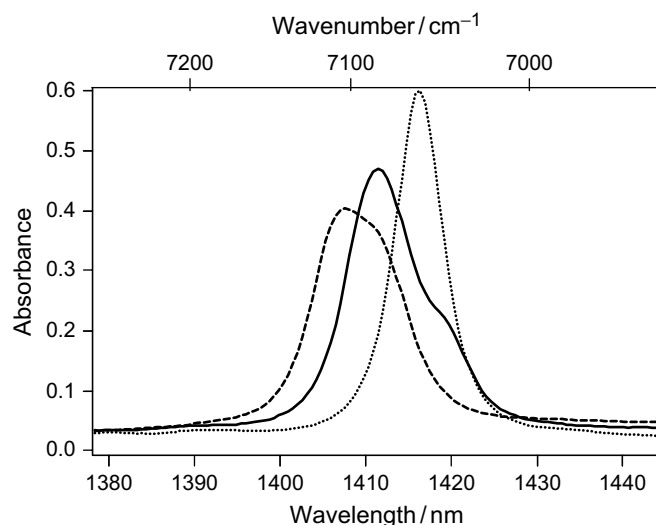


**Figure 8.** Shift of the hydroxyl first overtone in alcohols: (---) 1-butanol; (—) 2-butanol; (····) *t*-butanol.

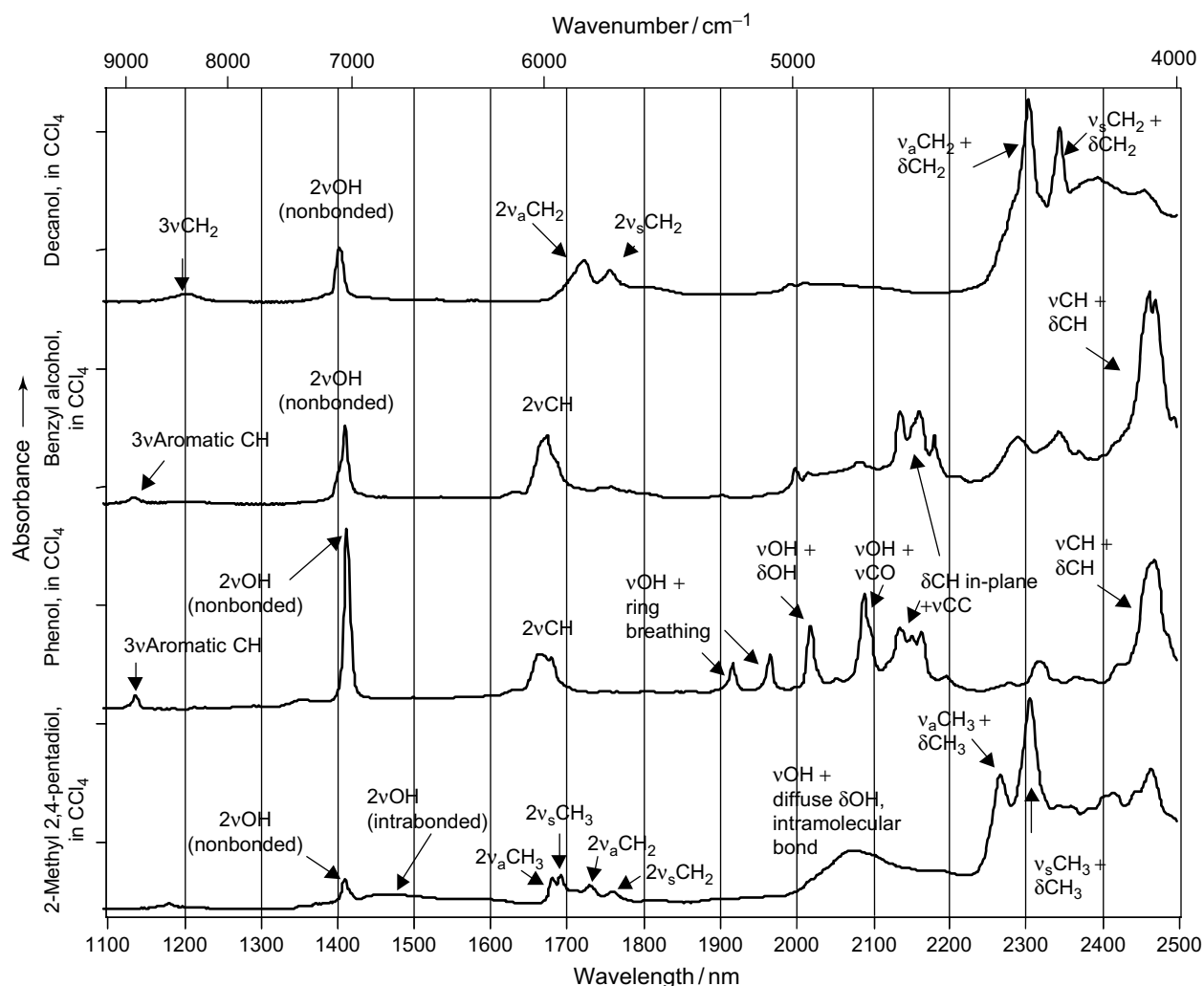


**Figure 9.** NIR spectra of hydroxyl-containing compounds.

model species. Rospenk *et al.*<sup>57</sup> compared the spectra of phenol and phenol-OD to show that a series of strong combination bands between 1920-nm ( $5210\text{ cm}^{-1}$ ) and 2100 nm ( $4760\text{ cm}^{-1}$ ) all involve the hydroxyl group, but no CH. The 1920-nm ( $5209\text{ cm}^{-1}$ ) and 1970-nm ( $5080\text{ cm}^{-1}$ ) peaks were assigned to OH stretch plus interactions with the ring, the 2020 nm ( $4949\text{ cm}^{-1}$ ) to OH stretch plus OH deformation, and the 2055-nm ( $4867\text{ cm}^{-1}$ ) and 2091-nm ( $4783\text{ cm}^{-1}$ ) peaks were probably due to OH stretch plus C–O stretches with some interactions with other vibrations.<sup>54</sup>

### 4.3 Multiple hydroxyl compounds

Glycols and other compounds having more than one hydroxyl have the opportunity for different types of hydrogen bonding. These include many natural compounds,

such as sucrose, starch, and cellulose, which will not be discussed thoroughly here.

Even in dilute solution, a diol will show an intramolecularly hydrogen-bonded hydroxyl peak.<sup>58</sup> Both bonded and nonbonded peaks are observed. The spectrum of 2-methyl-2,4-pentanediol in Figure 9 shows a nonbonded peak at 1415 nm ( $7065\text{ cm}^{-1}$ ) and an intramolecularly bonded peak at about 1460 nm ( $6850\text{ cm}^{-1}$ ). A small 1570-nm ( $6370\text{ cm}^{-1}$ ) intermolecularly bonded peak also appears. Based on information from the fundamental region, the spacing between the nonbonded and the intramolecularly bonded peaks increases with the number of carbon atoms between the two hydroxyls.<sup>11,58</sup>

Carbohydrates in general may have a free OH stretch absorption near 1440 nm ( $6940\text{ cm}^{-1}$ ). This band has been reported in crystalline sucrose, for example, and has been assigned specifically to the C<sub>4</sub> hydroxyl within a crystalline matrix.<sup>59</sup>

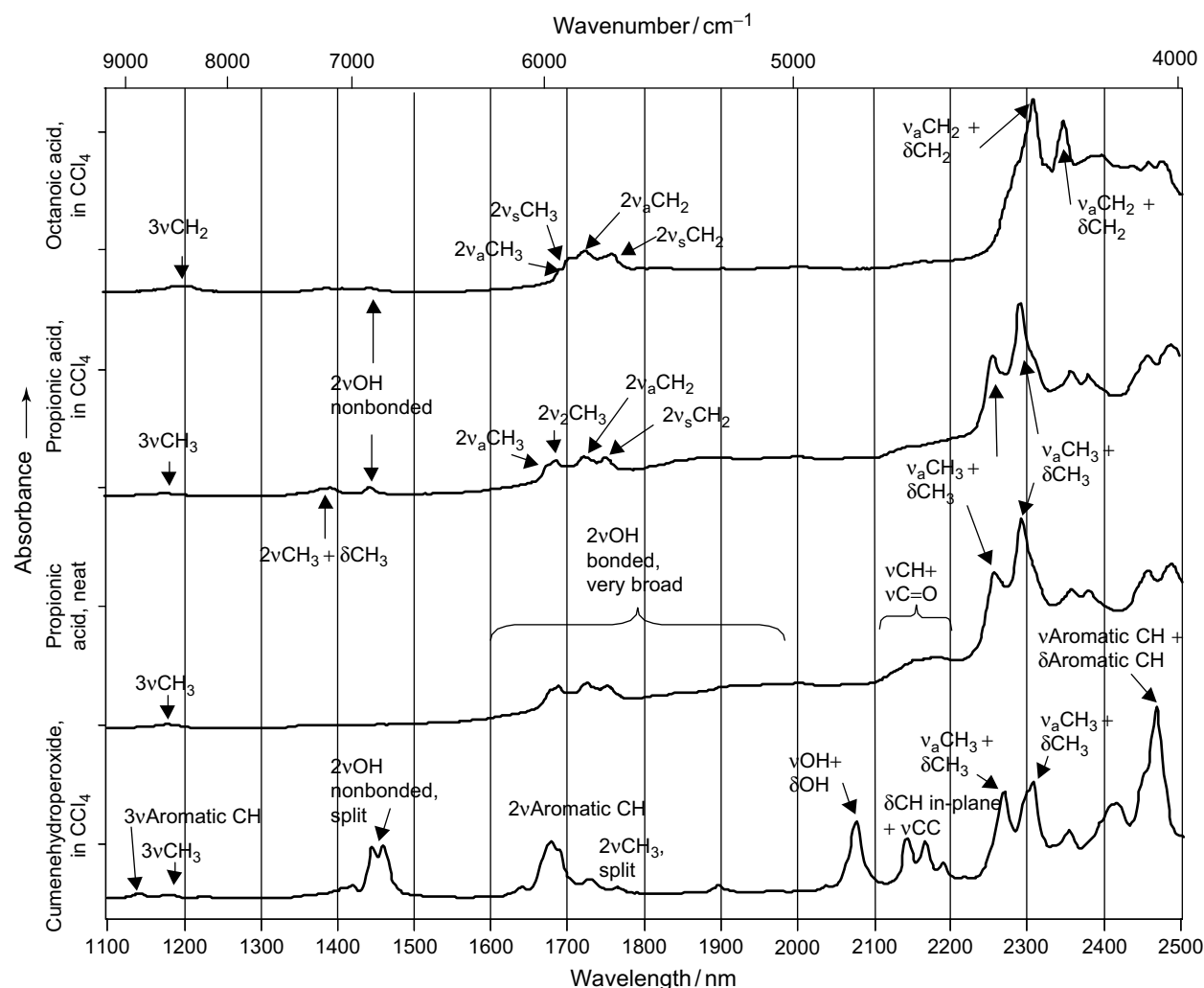


Figure 10. NIR spectra of carboxylic acids and a hydroperoxide.

#### 4.4 Carboxylic acids

The OH group associated with monomeric carboxylic acid has a sharp nonbonded or free stretching first overtone at about 1445 nm ( $6920\text{ cm}^{-1}$ ). This is shown in the spectra of oleic and octanoic acids in carbon tetrachloride in Figure 10. This band has also been observed in the high-temperature ( $92^\circ\text{C}$ ) spectrum of octanoic acid.<sup>60</sup> As seen in the figure, there is some overlap of this band with CH combination bands. This overlap appears more pronounced in acids than in alcohols because the acid hydroxyl absorptivity is significantly lower than the alcohol absorptivity. As the temperature is lowered or the solution becomes more concentrated, the formation of dimers with hydrogen-bonded hydroxyl groups broadens the OH stretch overtone and moves it to a longer wavelength (lower frequency) as it does in the MIR. This is illustrated in Figure 11, a temperature series. Although one can usually

observe the broad dimeric hydroxyl band in the MIR, in the NIR it appears only to shift the baseline upward in the region from about 1700 nm to at least 2200 nm. Spectral subtraction reveals a very broad and shallow curve in this region.

The second overtone of the nonbonded carboxylic acid hydroxyl is at about 1000 nm ( $10\,000\text{ cm}^{-1}$ ), and the third at about 800 nm ( $12\,500\text{ cm}^{-1}$ ).<sup>13</sup>

A peak near 1890 nm due to OH stretch combined with C=O stretch is readily observable in Figure 10 and the high-temperature curves of Figure 11. Also, a doublet at about 2130 nm ( $4695\text{ cm}^{-1}$ ) and 2160 nm ( $4630\text{ cm}^{-1}$ ) can be seen. This is due to a CH stretch and C=O stretch combination and has been split because of a rotational mode.

Other, smaller features in the spectrum of monomeric carboxylic acids observed in the gaseous state<sup>61</sup> include small peaks near 1220 nm ( $8200\text{ cm}^{-1}$ ) due to a combination

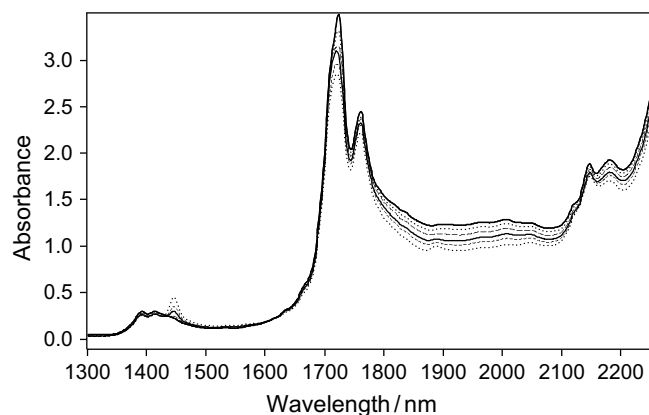


**Figure 11.** Spectral changes in the acid hydroxyl that occur with temperature. The dotted curve is the highest temperature.

between the first overtone of the OH stretch and a COH bending mode, 1240 nm ( $8070\text{ cm}^{-1}$ ) due to the first overtone of the OH stretch and the CO stretch, 1315 nm ( $7600\text{ cm}^{-1}$ ) due to the first overtone of the OH stretch and OCO bending, and 1540 nm ( $6500\text{ cm}^{-1}$ ) due to OH stretch and CH stretch.

Additional small peaks include those at about 2020 nm ( $4950\text{ cm}^{-1}$ ), a combination of the OH stretch and CH bending; 2080 nm ( $4800\text{ cm}^{-1}$ ), the combination of OH stretch and COH bending; 2120 nm ( $4710\text{ cm}^{-1}$ ), the combination of CH stretch and C=O stretch; 2140 nm ( $4680\text{ cm}^{-1}$ ), the combination of OH stretch and CO stretch; 2380 nm ( $4210\text{ cm}^{-1}$ ), the combination of OH stretch and OCO bending; 2390 nm, the combination of CH stretch and COH bending; and 2470 nm ( $4050\text{ cm}^{-1}$ ), the combination of CH stretch and CO stretch. All of these assignments are for formic acid in the gaseous state. Acids with more complex hydrocarbon structures would have more combination bands, and the region from 2200 to 2500 nm can become quite complex.

Spectra of dimeric carboxylic acids have a different set of small peaks due to the shifts in the OH and C=O structures. In the gaseous spectrum of formic acid, small peaks appear at about 1780 nm ( $5630\text{ cm}^{-1}$ ) due to a combination of CH stretch, CH bending, and CO stretch; 2130 nm ( $4700\text{ cm}^{-1}$ ) due to a combination of C=O stretch and CH stretch; 2220 nm ( $4500\text{ cm}^{-1}$ ) due to OH stretch and OH–O bending; 2240 nm ( $4460\text{ cm}^{-1}$ ) due to OH stretch and CH bending; 2300 nm ( $4340\text{ cm}^{-1}$ ) due to CH stretch and OH–O bending; 2320 nm ( $4310\text{ cm}^{-1}$ ) due to OH stretch and CO stretch; and 2400 nm ( $4160\text{ cm}^{-1}$ ) due to CH stretch and COH bending.

#### 4.5 Hydrogen peroxides

The first overtone of the nonbonded hydroxyl peak of a hydroperoxide in dilute solution is far enough removed

from that of acids and alcohols such that it can be used for quantitative analysis.<sup>11</sup> The peak is at about 1460 nm ( $6850\text{ cm}^{-1}$ ) as compared with 1410 nm ( $7100\text{ cm}^{-1}$ ) for alcohols. The spectrum of cumyl hydroperoxide shown in Figure 10 shows a splitting of the hydroxyl peak due to interaction with the benzene ring.<sup>11</sup> This doublet changes to a singlet in methylene chloride. There is also a combination band, which probably involves the OH stretch and OH bending at about 2060 nm ( $4850\text{ cm}^{-1}$ ), again in dilute solution. These two bands were found to be characteristic of hydrogen peroxides in dilute carbon tetrachloride solutions of fatty acids.<sup>62</sup> The combination band near 2060 nm can also be observed in neat hydrogen peroxide, as seen in Figure 12.

High overtones of the OH stretch, such as the fifth at 619 nm and the sixth at 532 nm, have been used in studying photoactivated dissociation of *t*-butyl hydroperoxide.<sup>63</sup> Excitation at these wavelengths creates a vibrationally hot electronic ground state.

## 5 WATER

### 5.1 Liquid water, ice, and water vapor

A summary of the absorption bands of water in the 800–2500 nm region is provided in Table 1.<sup>64</sup> Spectra of water in various media are shown in Figures 12 and 13. The vapor spectral details shown in the table were probably taken from a low-resolution spectrum, as a much larger number of water vapor peaks have been reported by others.<sup>65</sup> As shown in the table, the accepted assignments for the two bands at about 1450 nm ( $6900\text{ cm}^{-1}$ ) and 970 nm ( $10\,300\text{ cm}^{-1}$ ) indicate that these are combination bands involving the symmetric and asymmetric stretching modes of the water molecule. This observation has been made by comparison with high-resolution vapor spectra, which show that the combination bands are stronger than the overtones of either the symmetric or asymmetric stretch.<sup>66</sup> This assignment is further supported by consideration of the symmetry group of the vibrations.<sup>67</sup> It has also been suggested that the first overtone of the asymmetric stretch is accidentally degenerate with the sum of asymmetric and symmetric stretches in dilute solutions.<sup>68</sup> These two bands are generally referred to as the first and second overtones of the OH stretch, although that statement is not exactly true. The strong 1940-nm ( $5150\text{ cm}^{-1}$ ) peak is a combination of the asymmetric stretch and bending of the water molecule.

The water peaks with maxima near 970 nm<sup>69</sup> ( $10\,300\text{ cm}^{-1}$ ), 1200 nm ( $8330\text{ cm}^{-1}$ ),<sup>66,70</sup> and 1450 nm ( $6900\text{ cm}^{-1}$ ) at room temperature shift towards lower wavelength (higher wavenumber) with increasing temperature,

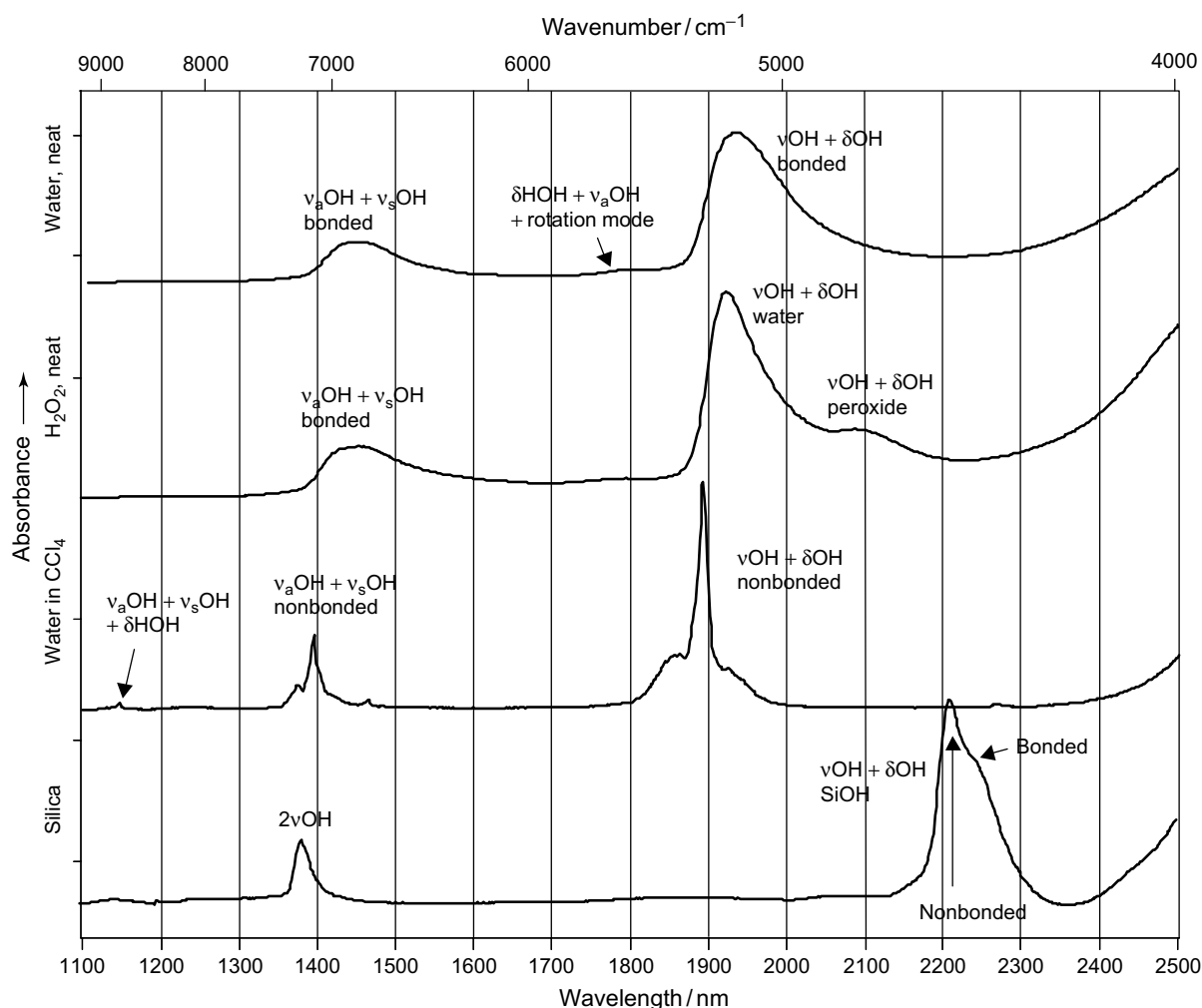


**Figure 12.** NIR spectra of water and related chemical species.

**Table 1.** Absorption peaks of water.

Ice (nm)	Ice (cm <sup>-1</sup> )	Liquid near freezing point (nm)	Liquid near freezing point (cm <sup>-1</sup> )	Liquid near boiling point (nm)	Liquid near boiling point (cm <sup>-1</sup> )	Vapor (nm)	Vapor (cm <sup>-1</sup> )	Assignment
800	12 500	770	13 000	740	13 500	723	13 831	3v <sub>1</sub> + v <sub>3</sub>
909	11 000	847	11 800	840	11 900	823	12 151	2v <sub>1</sub> + v <sub>2</sub> + v <sub>3</sub>
1025	9760	979	10 210	967	10 340	942	10 613	2v <sub>1</sub> + v <sub>3</sub>
1250	7990	1200	8310	1160	8640	1135	8807	v <sub>1</sub> + v <sub>2</sub> + v <sub>3</sub>
1492	6700	1453	6880	1425	7020	1380	7252	v <sub>1</sub> + v <sub>3</sub>
1780	5620	1780	5620	1786	5600	—	—	v <sub>2</sub> + v <sub>3</sub> + v <sub>L</sub>
1988	5030	1938	5160	1916	5220	1875	5332	v <sub>2</sub> + v <sub>3</sub>

v<sub>1</sub> is the symmetric stretch of the water molecule, v<sub>2</sub> is the bending mode, and v<sub>3</sub> is the asymmetric stretch. v<sub>L</sub> was not defined in the original reference, but is probably the hindered rotation near 600 cm<sup>-1</sup>.

and appear to consist of an unresolved pair of peaks with an isosbestic point between them. The isosbestic point for the 970-nm band is 990 nm (10 100 cm<sup>-1</sup>), for the 1200-nm band (8330 cm<sup>-1</sup>) about 1190 nm (8400 cm<sup>-1</sup>),<sup>66</sup> and for the 1450-nm band about 1440 nm (6960 cm<sup>-1</sup>).<sup>67</sup> The

presence of an isosbestic point indicates that NIR calibrations for water independent of temperature may be possible by judicious wavelength choice.

There has been some controversy over whether liquid water contains water molecules in three states of hydrogen



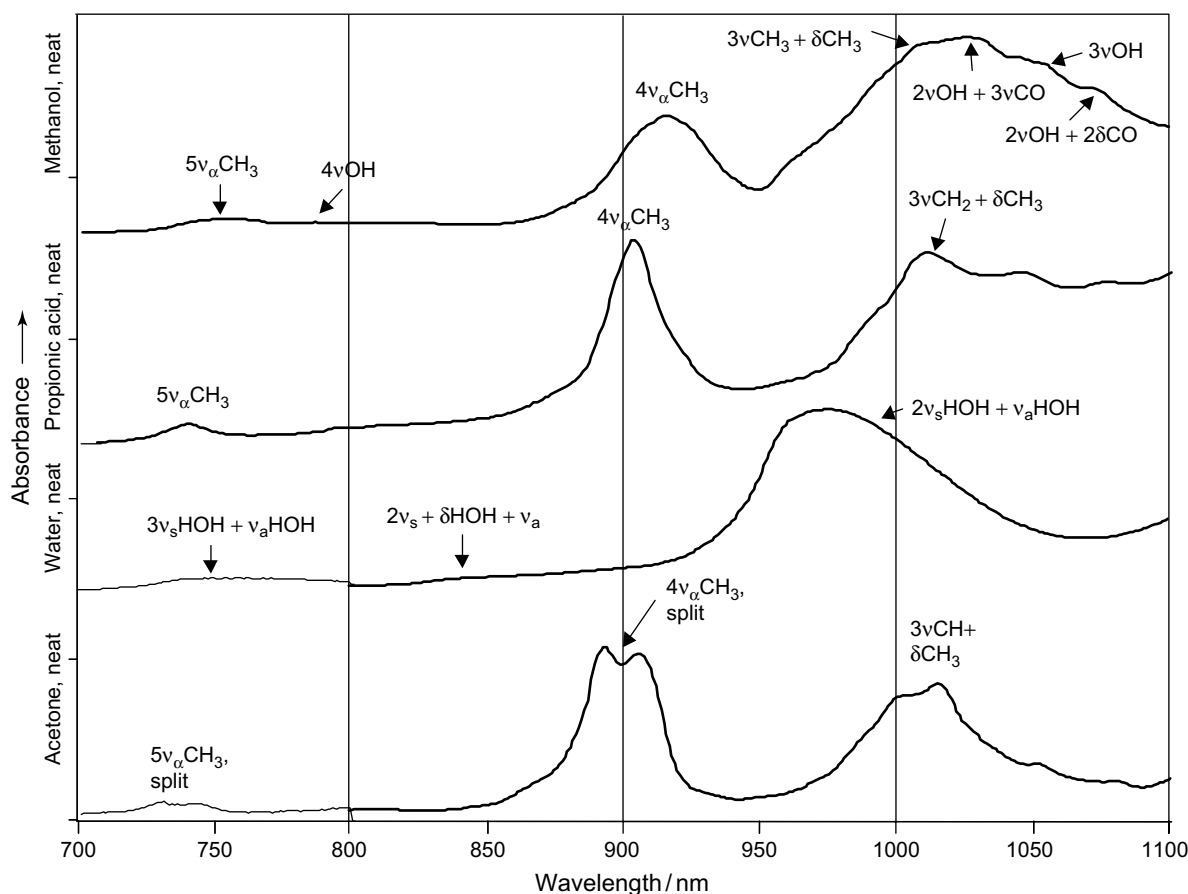


**Figure 13.** NIR spectra of selected hydroxyl- and carbonyl-containing compounds in the short-wavelength region.

bonding: free, bonded through one, two, or three hydrogen bonds, or a continuum of different bond strengths or somewhere in between.<sup>70</sup> In general, temperature studies and data treatments such as second derivatives and spectral resolution have indicated that there are separate peaks present for different states of hydrogen-bonded water molecules.<sup>71</sup> As pointed out by Maeda *et al.*<sup>71</sup> the intensities and width of these peaks are affected by the anharmonicity of each, so that the molecules bonded to more adjacent molecules, having less anharmonicity, will be broader and weaker.

## 5.2 Water in various solvents

The structure of water, and the band assignments of water in various solvents, has been studied extensively in the NIR. The 1940-nm ( $5155\text{ cm}^{-1}$ ) combination band in particular has been very useful for studies and analyses of water in the presence of hydroxyl-containing solvents because it is usually well isolated.

The position and widths of the bands vary predictably with the degree of hydrogen bonding and the basicity of the solvent.<sup>72</sup> Interactions are strongest in dimethyl sulfoxide

(DMSO) and weakest in nitromethane, as demonstrated by the position of the 1940-nm peak. The series of solvents includes, in order, DMSO, dioxane, acetone, acetonitrile, and nitromethane, and the peak maximum ranged from 1942 nm ( $5150\text{ cm}^{-1}$ ) to 1898 nm ( $5270\text{ cm}^{-1}$ ).<sup>73</sup> The effect of low levels of ethanol added to water was seen to be qualitatively the same as a temperature effect.<sup>74</sup>

In all solvents, the fraction of free water was greater in both dilute solution and in neat water than it was in intermediate concentrations. Through the analysis of ternary mixtures, the amount of nonbonded water molecules was found to be negligibly small in proton-acceptor solvents.

## 5.3 Water in other matrices, including glasses

The relative position of the water bands and sub-bands has provided a good deal of information to researchers. In studying protein denaturation, for example, the symmetric stretch + asymmetric stretch combination band provided information on the state of the water during the reaction. The shift from 1410 to 1490 nm indicated an increase in bound water.<sup>75</sup> In studying water sorption on PET film, the

same spectral region showed that water was not interacting with the film. The wavelengths of the sub-bands in that region were all lower than those in bulk water.<sup>76</sup> The total water content of starch and cellulose was compared with the “water activity” using the 1450- and 1940-nm bands.<sup>77</sup> It was found that NIR could discriminate between different levels of moisture content at the same activity, but not very well between activities at the same moisture content. The 1940-nm band was also used in a cell adhesion study.<sup>78</sup>

Water incorporated into fused silica is of considerable importance because the resulting silanol groups affect the NIR transmission of silica optical fibers and other optical components. The first overtone of the OH stretch of a silanol group in fused silica optical fibers is at about 1390 nm ( $7200\text{ cm}^{-1}$ ).<sup>79</sup> This band has been resolved into four peaks, two major and two minor, representing three different OH stretch peaks in different environments and one combination with a  $280\text{ cm}^{-1}$   $\text{SiO}_2$  fundamental that is Raman active. The second overtone shows a similar pattern centered at about 940 nm ( $10\,600\text{ cm}^{-1}$ ), and the third near 725 nm ( $13\,800\text{ cm}^{-1}$ ). Combination band assignments given by Stone and Walrafen<sup>79</sup> for bands at 2440 nm ( $4100\text{ cm}^{-1}$ ), 2250 nm ( $4450\text{ cm}^{-1}$ ), and 2210 nm ( $4520\text{ cm}^{-1}$ ) involve an OH stretch with one of the  $\text{SiO}_2$  fundamentals. Combinations involving twice the frequency of an OH stretch with the SiO stretch near  $800\text{ cm}^{-1}$  were noted at 1260 nm ( $7920\text{ cm}^{-1}$ ) and 1240 nm ( $8065\text{ cm}^{-1}$ ), and one band at three times an OH stretch plus the  $800\text{ cm}^{-1}$  band was observed at 850 nm ( $11\,500\text{ cm}^{-1}$ ). In mixed glasses, such as those containing borosilicates, aluminosilicates, etc., associated OH groups give rise to diffuse absorption bands.<sup>80</sup> The absorption bands of water molecules on silica surfaces has been described by Klier *et al.*<sup>81</sup>

## 5.4 Ionic species in water

An ionic hydroxyl group in aqueous solutions exhibits first and second overtone bands at 1421 nm ( $7040\text{ cm}^{-1}$ ) and 967 nm ( $1034\text{ cm}^{-1}$ ).<sup>82,83</sup> Also, a broad band centered at about 1100 nm has been attributed to the binding of two water molecules to the hydroxide ion.<sup>83</sup> As the hydroxide concentration is increased above 5 molal, the bulk water peaks at 1450 nm ( $6900\text{ cm}^{-1}$ ) and 976 nm ( $1025\text{ cm}^{-1}$ ) decrease, and the hydroxide ion peaks at 1421 and 967 nm, become prominent. This effect is complicated, however, and involves water activity and the ability of the solutes to confine the bulk solvent within hydration spheres. KOH solutions do not behave in the same way as NaOH solutions, and the effects of the cation on the water absorption need to be accounted for to obtain good measurements of hydroxide.

Sodium chloride alone in water can be measured readily in spite of its having no NIR bands of its own, because it affects the spectrum of water by reducing the amount of hydrogen bonding within the bulk water.<sup>84,85</sup> Different ions would have somewhat different effects, depending on their size and electronic characteristics. Divalent magnesium ions, trivalent aluminum ions, and protons, for example, enhance the structural order of the water, while monovalent sodium and potassium disrupt it.<sup>86</sup> Also, hydroxide and fluoride anions enhance the structure, while chloride, bromide, nitrite, and isocyanate disrupt it.<sup>87</sup> Choppin and Buijs<sup>87</sup> based their assessment of structure effects on the 1200-nm ( $8330\text{ cm}^{-1}$ ) combination band by calculating the relative intensities of the free, singly-bonded, and doubly-bonded peaks. Measurement of pH and titration endpoints by NIR based on the effects on the water peaks have been reported.<sup>86</sup>

## 6 CARBONYL COMPOUNDS

Aldehydes, ketones, esters, anhydrides, acid chlorides and carboxylic acids show also some NIR bands, as illustrated in Figure 14. The C=O stretch is very strong in the MIR, so even though the first overtone is still in the MIR region, the second overtone may be strong enough to observe in the NIR. Although the second overtones are relatively weak and would be overwhelmed by any water absorption, there are several anhydrous situations in which the carbonyl bands may be useful. These would include some polymers such as acrylic esters, neat ketones, anhydrides, and acid chlorides. In the latter two situations, any water would react with the anhydride or acid chloride to form acid, and there would not, therefore, be any water present.

As in the MIR, the position of the C=O varies with the environment of the group. In general, the position of the second overtone of simple noncyclic aliphatic compounds shifts to lower wavelength in the series: acid chlorides, anhydrides, carboxylic acid monomer, lactones, aldehydes, ketones, and esters. Amide carbonyl second overtones are overwhelmed by bands that involve NH stretch and cannot therefore be included in this comparison. An acid chloride second overtone is at 1850 nm ( $5400\text{ cm}^{-1}$ ), propionaldehyde is at 1960 nm ( $5100\text{ cm}^{-1}$ ), acetone is at 1960 nm ( $5100\text{ cm}^{-1}$ ) [with an additional split band at 1900 nm ( $5260\text{ cm}^{-1}$ )], and ethyl acetate is at 1940 nm ( $5160\text{ cm}^{-1}$ ). Conjugation with aromatic rings and double bonds, and interactions with halogens and cyclic structures, all affect the band positions, as in the MIR. Also, there is some question as to whether these second overtones are split into two, as there may be two or more small bands in the vicinity of the calculated second overtone.<sup>88</sup> The second overtone

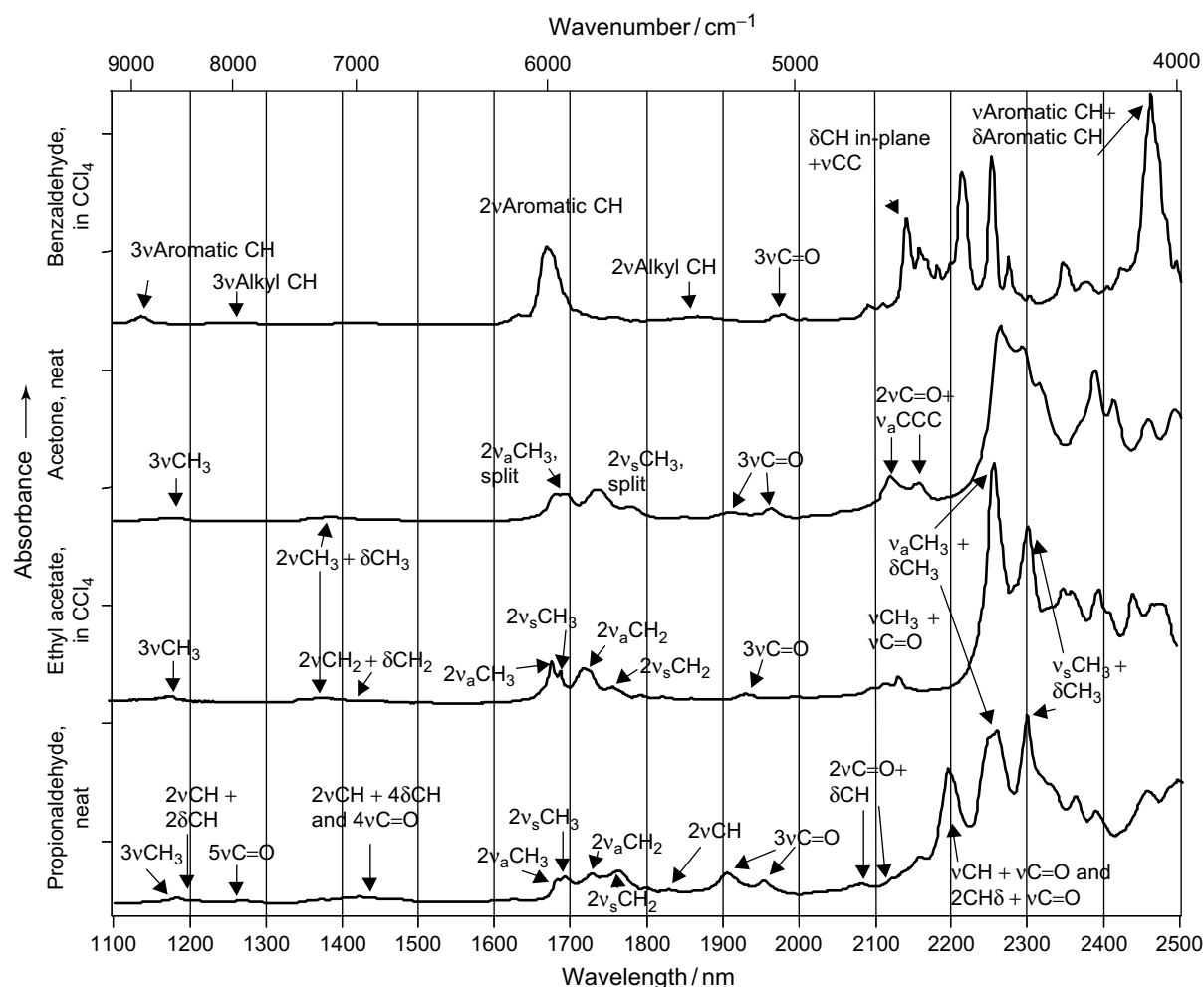


**Figure 14.** NIR spectra of selected carbonyl-containing compounds.

of the C=O of a carboxylic acid appears at about 1900 nm ( $5260\text{ cm}^{-1}$ ) and is particularly clear in a spectrum of perfluorocaproic acid taken in solution, as this acid has no CH absorptions.<sup>89</sup>

In addition to the overtones, there are some combination bands that include the C=O stretch. Combination bands involving C=O and CH in ketones are weak, if they exist at all, because the two groups do not share a common carbon atom. In aldehydes and formates, however, there is an H–C=O structure, and a corresponding combination band in the region of 2100–2200 nm ( $4760\text{--}4445\text{ cm}^{-1}$ ).<sup>3,89</sup> The strong formate ester band at 2150 nm ( $4650\text{ cm}^{-1}$ ) was assigned to CH stretch and C=O stretch by a deuteration study.<sup>90</sup>

In short-chain aliphatic aldehydes, bands at 2045 nm ( $4888\text{ cm}^{-1}$ ) and 2106 nm ( $4748\text{ cm}^{-1}$ ) were assigned as  $2 \times \text{C=O}$  stretch plus CH bending.<sup>91</sup> Also, a combination CH stretch and C=O stretch was observed at 2220 nm ( $4504\text{ cm}^{-1}$ ), along with a combination  $2 \times \text{CH}$  bend and C=O stretch at 2215 nm ( $4514\text{ cm}^{-1}$ ).<sup>92</sup>

The CH stretch overtones of aldehydes are at longer wavelengths than most compounds, as they are in the MIR. Thus, as shown in Figure 14, the CH stretch of benzaldehyde's alkyl is at 1860 nm ( $5376\text{ cm}^{-1}$ ).<sup>93</sup> It is very weak, possibly due to perturbation by a combination band.

## 7 MISCELLANEOUS

The spectral features of vibrations of haloalkanes are affected by the mass of the halogen atom and the force constant of the carbon–halogen bond. If a halogen is bound to the same carbon atom as the hydrogen, the neighboring CH overtone bands are shifted to shorter wavelength and their intensities are intensified.<sup>10</sup> The characteristic absorptions of hydrogen and other atoms should be detectable in the NIR region. Goddu<sup>11</sup> observed a weak S–H first overtone band from benzenethiol and 1-butanethiol at 1970–1980 nm ( $5076\text{--}5051\text{ cm}^{-1}$ ). In contrast, on the investigation of ethanethiol and dimethylaminoethanethiol, the band at

1740 nm ( $5747\text{ cm}^{-1}$ ) was assigned to the first overtone of S–H stretching.<sup>94</sup>

The first overtone of P–H stretching is found at 1892 nm ( $5258\text{ cm}^{-1}$ ) from a number of organophosphorus compounds. This weak diffuse band could be useful for qualitative purposes. The POH absorptions could be observed in phosphorothioic acids, which shifts to 1908 nm as compared with normal hydroxyl overtones. The effect of hydrogen bonding in phosphorus acids causes this displacement. The group of phosphorus-thiol (P–SH) also shows a shift from the normal thiol overtone and gives rise to a weak doublet at 1970 and 1999 nm ( $5076\text{--}5002\text{ cm}^{-1}$ ). In studies of wavelength displacement of deuterium substitution, hexadeuteropropylene ( $\text{CD}_3\text{CD}=\text{CD}_2$ ) gives a asymmetric stretching of the  $\text{CD}_2$  at 2170 nm. In an aromatic system, hexadeuterobenzene ( $\text{C}_6\text{D}_6$ ) has bands at 1900, 1560, 1375 and 1010 nm, which correspond to the first, second, third and forth overtones of C–D stretchings, respectively.<sup>3</sup>

## ACKNOWLEDGMENTS

The authors would like to thank Dongsheng Bu at the University of Rhode Island for obtaining some of the spectra and James P. Malone of Genesis Associates for the acid temperature series spectra.

## ABBREVIATIONS AND ACRONYMS

DMSO Dimethyl Sulfoxide

## REFERENCES

- U. Bernhard and P.H. Berthold, *Jena Rev.*, **20**(5), 248 (1975).
- D.L. Snavely and C. Angevine, *J Polym. Sci., Part A: Polym. Chem.*, **34**(9), 1669 (1996).
- W. Kaye, *Spectrochim. Acta*, **6**, 257 (1954).
- I. Murray and P.C. Williams, 'Chemical Principles of Near-infrared Technology', in "Near-infrared Technology in the Agricultural and Food Industries", eds P. Williams and K. Norris, American Association of Cereal Chemists, St Paul, MN, 17–34, Chapter 2 (1987).
- L.G. Weyer, *Appl. Spec. Rev.*, **21**(1&2), 1 (1985).
- F.H. Lohman and Norteman, *Anal. Chem.*, **35**(6), 707 (1963).
- R.B. Stage, J.B. Stanley and P.B. Moseley, *J. Am. Oil Chem. Soc.*, **49**, 87 (1972).
- T. Hirschfeld and A.Z. Hed (eds), 'The Atlas of Near Infrared Spectra', Sadtler Research Laboratories, Philadelphia (1981).
- M. Buback and H.P. Voegelé, 'FT-NIR Atlas', VCH, Weinheim (1993).
- O. Wheeler, *Chem. Rev.*, **59**, 629 (1959).
- R. Goddu, *Adv. Anal. Chem.*, **1**, 347 (1960).
- K.B. Whetsel, *Appl. Spectrosc. Rev.*, **2**(1), 1 (1968).
- J.J. Workman, *Appl. Spectrosc. Rev.*, **31**(3), 251 (1996).
- B.G. Osborne and T. Fearn, 'Near Infrared Spectroscopy in Food Analysis', Longman Scientific and Technical, Harlow (1986).
- M.A. Czarnecki, H. Maeda, Y. Osaki, M. Suzuki and M. Iwahashi, *Appl. Spectrosc.*, **52**(7), 994 (1998).
- F.B. Barton, D.S. Himmelsbach, J.H. Duckworth and M.J. Smith, *Appl. Spectrosc.*, **46**, 420 (1992).
- F.B. Barton and D.S. Himmelsbach, *Appl. Spectrosc.*, **47**, 1920 (1993).
- I. Noda, Y. Liu, Y. Ozaki and M.A. Czarnecki, *J. Phys. Chem.*, **99**, 3068 (1995).
- C. Tosi and A. Pinto, *Spectrochim. Acta*, **28A**, 585 (1972).
- A.S. Bonanno and P.R. Griffiths, *J. Near Infrared Spectrosc.*, **1**, 13 (1993).
- A.S. Wexler, *Anal. Chem.*, **40**, 1868 (1968).
- M.S. Child, *Acc. Chem. Res.*, **18**, 45 (1985).
- J.L. Duncan, *Spectrochim. Acta*, **47A**, 1 (1991).
- L. Ricard-Lespade, G. Longhi and S. Abbate, *Chem. Phys.*, **142**, 245 (1990).
- L.N. Lewis, *J. Organomet. Chem.*, **234**, 355 (1982).
- M. Avram and Gh.D. Mateescu, 'Infrared Spectroscopy, Applications in Organic Chemistry', Wiley-Interscience, New York, 202 (1970).
- D. Bassi, L. Menegotti, S. Oss, M. Scotoni and F. Iachello, *Chem. Phys. Lett.*, **207**, 167 (1993).
- T. Luty and J.W. Rohleder, *Roczniki Chemi.*, **41**, 975 (1967).
- T.V.K. Sarma, C.V.R. Sastry and C. Santhamma, *Spectrochim. Acta*, **43A**, 1059 (1987).
- K.V. Reddy, D.F. Heller and M.J. Berry, *J. Chem. Phys.*, **76**, 2814 (1982).
- R. Bini, P. Foggi and R.G. Della Valle, *J. Phys. Chem.*, **95**, 3027 (1991).
- D.L. Snavely, J.A. Overly and V.A. Walters, *Chem. Phys.*, **201**, 567 (1995).
- R.J. Proos and B.R. Henry, *J. Phys. Chem. A*, **103**, 8762 (1999).
- E.D. Yalvac, M.B. Seasholz and S.R. Crouch, *Appl. Spectrosc.*, **51**, 1303 (1997).
- P.G. Gassman and W.M. Hooker, *J. Am. Chem. Soc.*, **87**, 1079 (1965).
- R.T. Holman and P.R. Edmondson, *Anal. Chem.*, **28**, 1533 (1956).
- L.A. Strait and M.K. Hrenoff, *Spectrosc. Lett.*, **8**, 165 (1975).
- R.T. Conley, 'Infrared Spectroscopy', Allyn and Bacon, Boston, Chapter 7 (1966).
- J.E. Sinsheimer and A.M. Keuhnelian, *Anal. Chem.*, **46**, 89 (1974).
- F.H. Lohman and W.E. Norteman, *Anal. Chem.*, **35**, 707 (1963).

41. R.A. Russell and H.W. Thompson, *Proc. R. Soc. London*, **A234**, 318 (1956).
42. I. Murray, 'The NIR Spectra of Homologous Series of Organic Compounds', in "International NIR/NIT Conference", eds J. Hollo, K.J. Kaffka and J.L. Goenczy, Budapest, Hungary, 13–28 (1987).
43. K.B. Whetsel, *Spectrochim. Acta*, **17**, 614 (1961).
44. G. Durocher and C. Sandorfy, *J. Mol. Spectrosc.*, **22**, 347 (1967).
45. S.E. Krikorian and M. Mahpour, *Spectrochim. Acta*, **29A**, 1233 (1973).
46. K.T. Hecht and D.L. Wood, *Proc. R. Soc. London, Ser. A*, **235**, 174 (1956).
47. M. Czarnecki, H. Maeda, Y. Ozaki, M. Suzuki and M. Iwahashi, *J. Phys. Chem. A*, **102**, 9117 (1998).
48. L. England, D. Schloeberg and W.A.P. Luck, *J. Mol. Struct.*, **143**, 325 (1986).
49. C. Bourderon, J.J. Peron and C. Sandorfy, *J. Phys. Chem.*, **76**(6), 864 (1972).
50. A.M.C. Davies and S.G. Rutland, *Spectrochim. Acta*, **44A**(11), 1143 (1988).
51. C.L. Bell and G.M. Barrow, *J. Chem. Phys.*, **31**, 300 (1959).
52. L. England-Kretzer, M. Fritzsche and W.A.P. Luck, *J. Mol. Struct.*, **175**, 277 (1988).
53. H.L. Fang and R.L. Swofford, *Chem. Phys. Lett.*, **105**(1), 5 (1984).
54. S.B. Rai and P.K. Srivastava, *Spectrochim. Acta, Part A*, **55**, 2793 (1999).
55. N.B. Colthup, L.H. Daly and S.E. Wiberley, 'Introduction to Infrared and Raman Spectroscopy', Academic Press, New York (1990).
56. O.R. Wulf, E.J. Jones and L.S. Deming, *J. Chem. Phys.*, **8**, 753 (1940).
57. M. Rospenk, N. Leroux and T. Zeegers-Huyskens, *J. Mol. Spectrosc.*, **183**, 245 (1997).
58. W.A.P. Luck and W. Ditter, *J. Phys. Chem.*, **74**(21), 3687 (1970).
59. A.M.C. Davies and C.E. Miller, *Appl. Spectrosc.*, **42**(4), 703 (1988).
60. Y. Ozaki, Y. Liu, M.A. Czarnecki and I. Noda, *Macromol. Symp.*, **94**, 51 (1995).
61. S. Morita and S. Nagakura, *J. Mol. Spectrosc.*, **41**, 54 (1972).
62. R.T. Holman, C. Nickell and O.S. Privett, *J. Am. Oil Chem. Soc.*, **35**, 422 (1958).
63. D.W. Chandler and J.A. Miller, *J. Chem. Phys.*, **81**(1), 455 (1984).
64. H. Yamatera, B. Fitzpatrick and G. Gordon, *J. Mol. Spectrosc.*, **14**, 268 (1964).
65. O.L. Polyansky, N.F. Zobov, S. Viti and J. Tennyson, *J. Mol. Spectrosc.*, **189**, 291 (1998).
66. K. Buijs and G.R. Choppin, *J. Chem. Phys.*, **39**(8), 2035 (1963).
67. G.R. Choppin and M.R. Violante, *J. Chem. Phys.*, **56**(12), 5890 (1972).
68. G.R. Choppin and J.R. Downey, *J. Chem. Phys.*, **56**(12), 5899 (1972).
69. A. Inoue, K. Kojima, Y. Taniguchi and K. Suzuki, *J. Solution Chem.*, **13**(11), 811 (1984).
70. W.C. McCabe, S. Subramanian and H.F. Fisher, *J. Phys. Chem.*, **74**, 4360 (1970).
71. H. Maeda, Y. Ozaki, M. Tanaka, N. Hayashi and T. Kojima, *J. Near Infrared Spectrosc.*, **3**, 191 (1995).
72. Y.-S. Choi, 'Near Infrared Spectroscopic Investigations of Hydrogen-bonding of Water in Organic Solvents and Alcohols, and Partial Molal Volume Studies of Some Solutes in H<sub>2</sub>O and D<sub>2</sub>O', PhD dissertation, University of South Carolina (1974).
73. A. Burneau, *J. Mol. Liquids*, **46**, 99 (1990).
74. G. Onori, *Il Nuovo Cimento*, **10**(4), 387 (1988) (in English).
75. D.L. Vandermeulen and N. Ressler, *Arch. Biochem. Biophys.*, **205**(1), 180 (1980).
76. M. Fukuda, H. Kawai, N. Yagi, O. Kimura and T. Ohta, *Polymer*, **31**, 295 (1990).
77. S.R. Delwiche, R.E. Pitt and K.H. Norris, *Cereal Chem.*, **69**(1), 107 (1992).
78. D. Grant, W.F. Long and F.B. Williamson, 'NIR Spectroscopy Shows that Animal Cell Adhesion to Non-biological Solid Surfaces may Require Surface Water Structuring', in "Making Light Work", eds I. Murray and I.A. Cowe, VCH, Weinheim, 636–639 (1992).
79. J. Stone and G.E. Walrafen, *J. Chem. Phys.*, **76**(4), 1712 (1982).
80. G.A.C.M. Spierings, *Phys. Chem. Glasses*, **23**(4), 101 (1982).
81. K. Klier, J.H. Shen and A.C. Zettlemoyer, *J. Phys. Chem.*, **77**(11), 1458 (1973).
82. A. Heiman and S. Licht, *Anal. Chim. Acta*, **394**, 135 (1999).
83. M.K. Phelan, C.H. Barlow, J.J. Kelly, T.M. Jinguji and J.B. Callis, *Anal. Chem.*, **61**, 1419 (1989).
84. T. Hirschfeld, *Appl. Spectrosc.*, **39**, 740 (1985).
85. A. Grant, A.M.C. Davies and T. Bilverstone, *Analyst*, **114**, 819 (1989).
86. K. Molt, S. Berentsen, V.J. Frost and A. Niemoeller, *Spectrosc. Europe*, **10**(3), 16 (1998).
87. G.R. Choppin and K. Buijs, *J. Chem. Phys.*, **39**(8), 2042 (1963).
88. J.W. Ellis, *J. Am. Chem. Soc.*, **51**, 1384 (1929).
89. R.T. Holman and P.R. Edmondson, *Anal. Chem.*, **28**(10), 1533 (1956).
90. R.M. Powers, M.T. Tetenbaum and H. Tai, *Anal. Chem.*, **34**, 1132 (1962).
91. L. Kellner, *Proc. R. Soc. London*, **A157**, 100 (1936).
92. G. Lucazeau and C. Sandorfy, *Can. J. Chem.*, **48**, 3694 (1970).
93. P.K. Srivastava, G. Ullas and S.B. Rai, *Pramana J. Phys.*, **43**(3), 231 (1994).
94. R.A. McIvor, C.C. Hubley, G.A. Grant and A.A. Grey, *Can. J. Chem.*, **36**, 820 (1958).